

ON TRANSVERSE EFFECTS IN TRANSPORT IN SEMI- AND
SUPERCONDUCTORS

A Dissertation

by

KONSTANTIN SERGEEVICH TIKHONOV

Submitted to the Office of Graduate and Professional Studies of
Texas A&M University
in partial fulfillment of the requirements for the degree of

DOCTOR OF PHILOSOPHY

Chair of Committee,	A. M. Finkel'stein
Committee Members,	Ar. Abanov
	A. Belyanin
	G. Berkolaiko
	D. Naugle
Head of Department,	George Welch

December 2015

Major Subject: Physics

Copyright 2015 Konstantin S. Tikhonov

ABSTRACT

In this dissertation, the results obtained during my PhD work are presented. As an introduction, the brief review of the theory of superconducting fluctuations and a short discussion of experimental situation in the field of spin caloritronics are presented. Next, the original study of two important transport transverse effects is reported. The first one is the Hall effect in metallic films, enhanced by superconducting fluctuations. We develop an appropriate technique, based on solution of Usadel equation in the presence of classical and quantum noise and including leading contributions due to electron-hole asymmetry. This allows us to extend the previously known results for Cooper interaction-dominated transverse conductivity to a broader range of temperatures and magnetic fields, including the vicinity of the magnetic field induced quantum critical point. The second effect under study is Transverse Spin Seebeck Effect (TSSE). The TSSE remains one of the most puzzling of the recently discovered spin-dependent thermoelectric effects merging spin, charge, and thermal physics. We build a theory, which allows to quantitatively interpret the recent experimental results in terms of magnetized electrons, dragged but low-energy out-of-equilibrium phonons. The theory explains the manifestly non-local nature of the TSSE from the fact that phonons that store the energy (thermal) and the phonons that transfer it (subthermal) are located in different parts of the spectrum and have different kinetics. This gives rise to a spectral phonon distribution that deviates from local equilibrium along the substrate and is sensitive to boundary conditions. The theory also predicts a non-magnon origin of the effect in ferromagnetic metals in agreement with observations in recent experiments.

ACKNOWLEDGEMENTS

I am very grateful to my advisor, Alexander Finkel'stein for constant sharing of his encouragement and ideas with me. During my studies, he taught me many important things in physics and other matters of life.

I am also very grateful to Georg Schiwete, Karen Michaeli, Jairo Sinova, Wei Zhao for collaborations in which some parts of this work were done. The interesting discussions which this collaborations involved were always a pleasure.

I would like to thank the members of the Committee and Glenn Agnolett for their interest in my work and to all other participants of the Condensed Matter Seminar at TAMU for many insightful questions, in particular to Prof. V. L. Pokrovskii. I also acknowledge nice and stimulating discussions with members of Landau ITP: Igor Burmistrov, Michail Feigel'man and Michail Skvortsov. I'm also grateful to my friends in College Station: Aysen, Petya, Roman, Waldemar and many others. Finally, I thank my family for their constant support.

TABLE OF CONTENTS

	Page
ABSTRACT	ii
ACKNOWLEDGEMENTS	iii
TABLE OF CONTENTS	iv
LIST OF FIGURES	vi
1. INTRODUCTION	1
2. SUPERCONDUCTING FLUCTUATIONS IN THE FRAMEWORK OF USADEL EQUATION	4
2.1 Introduction	4
2.2 Basic equations	7
2.3 Solution of the Usadel equation and the order parameter correlation function	15
2.4 Fluctuation corrections: derivation	26
2.5 Discussion of the results for longitudinal conductivity	33
2.5.1 GL region (I)	34
2.5.2 Quantum critical point (II)	36
2.5.3 High temperatures (III) and high magnetic fields (IV)	38
2.6 Conclusion	42
3. HALL EFFECT IN SUPERCONDUCTING FILMS	45
3.1 Introduction	45
3.2 Particle-hole asymmetry and superconducting fluctuations	48
3.3 Discussion of the results for Hall conductivity due to superconducting fluctuations	51
3.4 Conclusion	54
4. TRANSVERSE SPIN SEEBECK EFFECT	55
4.1 Introduction	55
4.2 Physical mechanisms of the phonon-electron SSE	58
4.3 Subthermal phonon kinetics	61

4.4	Out of plane spin transport	65
4.5	Conclusion	70
5.	SUMMARY	73
	REFERENCES	74

LIST OF FIGURES

FIGURE	Page
2.1 Anomalous Maki-Thompson diagram	28
2.2 Phase Diagram for the correction to the longitudinal conductivity $\delta\sigma_{xx}$. The corresponding equations are written in the text.	33
2.3 Resistance as a function of temperature for magnetic fields $B/B_c = 0.9, 1.05, 1.1, 1.3$. The sample parameters are $R_D = 5k\Omega$ and $T_c\tau = 10^{-2}$	42
2.4 Resistance as a function of magnetic field for temperatures $T/T_c = 0.03, 0.1, 0.35$. Inset: the zoomed region of the approximate crossing for $T/T_c = 0.15 - 0.3$. The sample parameters are $R_D = 5k\Omega$ and $T_c\tau = 10^{-2}$	43
3.1 Phase diagram for the Hall effect: sign of the fluctuation correction to σ_{xy} coefficient is shown.	52
3.2 Hall effect in the superconducting films: experiment and theory.	53
4.1 Scheme of the SSE experiment. The effect incorporates three key physical mechanisms: (i) subthermal phonons whose inelastic length, l_{in} , is of the order of the sample size, L , and whose elastic length, l_{el} , is smaller than L , drive the non-local heat propagation along the substrate which gives rise to a steady state distribution function that deviates from local equilibrium; (ii) equilibration of heat flows out of the substrate into the Pt probe and backwards establishes the temperature in the probe $T_{Pt} \neq T(x)$; (iii) the different phonon distribution functions in the probe and the substrate yield a spin-phonon-drag current, $\vec{j}_s(x) \propto \delta T_{\perp}$	56
4.2 Spectral phase diagram of phonons as a function of sample length. The deviation from local thermal equilibrium, $\delta n(\omega, x) = n(\omega, x) - n_{T(x)}(\omega)$, is illustrated (green curve) for $x = L/3$; here $\rho_{ph}(\omega) \propto \omega^2$ is the phonon density of states.	57
4.3 Correction to the linear temperature dependence as a function of position, Eq. (4.12).	64

4.4 The function $H(x) \propto \delta T_{\perp}(x)$ determining the magnitude and spatial profile of the SSE signal S_{xy} given in Eq. (4.20). 67

1. INTRODUCTION

It would be fair to say that most of the transport studies of metals and semiconductors from both theoretical and experimental sides are devoted to determination of electrical and heat conducting properties of these materials. Normally, 'studying transport' means 'studying *longitudinal* transport'. The corresponding transport coefficients carry a lot of information about microscopic properties of the material under study. However, one quickly realises how important *transversal* effects can be: for example a sign of the charge of a current carrier e does not manifest itself in longitudinal conductivity of a material σ_{xx} , which is proportional to the charge squared $\sim e^2$. So, as soon as one is interested in the sign of e , he must turn to the study of transversal electric conductivity σ_{xy} , which behaves as $\sim e^3$. In addition, one quickly finds out that some noticeable contributions to σ_{xy} are proportional to the derivative of the density of states with respect to the energy at the chemical potential μ , a quantity which is not easy to infer by other means (the only other transport property that is sensitive to this quantity is the thermoelectric coefficient). Another example of importance of the transversal transport effects is the recently discovered Transversal Spin Seebeck Effect. In the conditions under which this effect is studied, transversality of the measured response is crucial as it allows to gain access to the physics of subthermal phonons which is not easily accessible in stationary situations. These two interesting pieces of physics (Hall effect in dirty metallic films and Transversal Spin Seebeck Effect) are central subjects of this work.

This thesis is organized as follows. In chapter 2, we present introduction to the history and main results of a theory of superconducting fluctuations. The main contribution of this chapter is generalization of the Usadel equation approach for

calculation of effects of both thermal and quantum superconducting fluctuations on transport properties of thin films[79]. We discuss how this approach allows to get all known result in this field in a simple and unifying manner.

In chapter 3, we apply the developed technique to calculate the effects of superconducting fluctuations on transversal electric conductivity. This implies taking into account the effects of particle-hole asymmetry in the propagator of Cooper interaction. We show that in the limit of weak interaction it can be done self-consistently in the framework of quasiclassical theory. Next, we use this method to calculate transversal conductivity σ_{xy} for a wide range of temperatures and magnetic fields, including the region of a quantum critical point at $T = 0$ [61]. Several asymptotical regimes are discussed and application of the theory to recent measurements is demonstrated [20].

In chapter 4, after introducing the basic experimental facts about the Transversal Spin Seebeck Effect, we motivate the necessity of more refined theoretical approach to this effect. In particular, we stress that the (i) non-local nature of the signal remains unexplained and (ii) observed dependence of transport coefficient S_{xy} on the magnetization M is not really consistent with previously proposed magnonic mechanism. Further on, we develop a theory which contributes to both of these subtle questions [80]. Building on top of kinetic theory of subthermal phonon propagation in insulators, we demonstrate possibility of phononic system alone to produce specific spatial profile of the signal. In addition, we argue that electron-phonon drag can serve as a force which generates spin current in the transversal direction which is then converted to electric voltage by a Pt probe. Finally, we demonstrate the qualitative agreement of the predictions of this theory with results of experiments on TSSE in various aspects.

The results presented in this work were reported on several seminars at Texas

A&M University (USA), as well as at Karlsruhe Institute of Technology, University of Mainz, Max Planck Institute for Solid State Research (Germany), Landau Institute for Theoretical Physics (Russia) and Weizmann Institute of Science (Israel).

2. SUPERCONDUCTING FLUCTUATIONS IN THE FRAMEWORK OF USADEL EQUATION*

2.1 Introduction

Theoretical studies of fluctuation conductivity in superconductors found their origin in the discovery of paraconductivity by Aslamazov and Larkin (AL) in 1968 [12]. These authors analyzed the conductivity of superconductors in the metallic phase above the transition temperature T_c in the framework of diagrammatic linear response theory. Paraconductivity can be understood as the direct contribution of fluctuating Cooper pairs to the electric current. Indeed, the formation of Cooper pairs opens a new channel for charge transport in the metallic phase. Above the transition temperature, these Cooper pairs do not form a condensate yet and their contribution to conductivity is positive but still bounded due to their finite lifetime. Other effects of superconducting fluctuations are Andreev scattering of electrons off the fluctuating order parameter described by the so-called Maki-Thompson (MT) term [60, 78], and the suppression of the quasiparticle density of states (DOS) near the Fermi-level.

These classical results were obtained for temperatures close to T_c and later extended for larger temperatures and for weak magnetic fields. More recently, the vicinity of the magnetic field-tuned quantum phase transition in disordered superconducting films was studied in a paper by Galitski and Larkin [30]. These authors have shown that close to the quantum transition, contrary to the previously studied regime of weak magnetic fields, different processes are of equal importance. This

*Part of this chapter is reprinted with permission from "Fluctuation conductivity in disordered superconducting films" by K. S. Tikhonov, G. Schwiete, A. M. Finkel'stein, 2012, Physical Review B 85 (17), 174527, Copyright (2012) by the American Physical Society.

has the remarkable consequence that the sign of the total correction to conductivity becomes negative for sufficiently low temperatures near the quantum critical point, resulting in a non-monotonic magnetoresistance in this regime.

In spite of the substantial amount of existing theoretical work on superconducting fluctuations, summarized in the book by Larkin and Varlamov [52], the subject continues to be an active field of research. This activity is stimulated by recent accurate experimental studies of different superconducting systems [37, 75, 14, 67, 48, 58], that call for refined theoretical studies. For example, when fitting experimental data on disordered superconducting films by theoretical results, one commonly uses several fitting parameters, including the critical temperature T_c , the upper critical field B_c and the dephasing time τ_ϕ . In doing so, it would be useful to work with theoretical results which are valid in the entire (B, T) phase diagram, instead of addressing different asymptotic regions separately. This is the motivation for our choice of Diffusive Usadel Equation is a main tool for this work.

In deriving the results for the fluctuation conductivity, we deviate from the traditional route that employs the diagrammatic linear response theory in the imaginary time technique [4] as described in detail, for example, in Ref. [52]. Instead, we develop a formalism based on the Keldysh (real-time) representation of the Usadel equation. In this approach, disorder averaging is performed at the earliest stages, thereby avoiding the use of the impurity-diagram technique. As an additional advantage, no analytic continuation is required. The Usadel equation [85] is an indispensable tool in the theory of mesoscopic superconductors and hybrid structures [16, 74]. This equation describes low-energy (diffusive) physics on spatial q^{-1} and temporal ω^{-1} scales, satisfying $(ql, \omega\tau) \ll 1$, where τ is the impurity scattering time and l the mean free path. The first calculation of superconducting fluctuation corrections in this framework was performed by Volkov et al. [89], who calculated fluctuation con-

ductivity in hybrid superconducting-normal structures in the vicinity of T_c in the absence of a magnetic field.

We use the Usadel equation to calculate longitudinal and transverse (Hall) conductivity in disordered superconducting films at arbitrary temperatures and magnetic fields. Our approach parallels to some extent the non-linear σ -model formalism for disordered superconductors introduced by Feigelman et al. [25], and the subsequent work by Kamenev and Levchenko [53]. The latter work includes a calculation of fluctuation conductivity close to T_c . The intimate relation between the σ -model formalism and the Usadel equation approach is based on the fact that the Usadel equation is the saddle point equation of the nonlinear σ -model. For the sake of simplicity, we decided not to use the more technical apparatus of the nonlinear σ -model, but formulate the derivation in terms of the Usadel equation. This route leads us to a description in terms of a coupled set of kinetic equations for quasiparticles moving on the background of superconducting fluctuations. This method appears to be a very convenient tool for studying fluctuation transport.

The classification of the fluctuation corrections obtained in the discussed method appears to be very different from the conventional classification based on the diagrams in the Matsubara technique. Therefore comparison with the results obtained by the diagrammatic technique can be performed only on the level of the final results. Let us mention here the comparison to recent works. It can be seen [77] that the zero magnetic field limit of the general formulas derived in this manuscript (Eqs. (2.89), (2.90), and (2.91) below) can be presented in a form that exactly coincides with the corresponding diagrammatic results of Lopatin et al. in Refs. [59, 73]. On the other hand, Glatz et al. more recently presented a diagrammatic analysis of the longitudinal fluctuation conductivity in the entire phase diagram [33, 32]. However, their results are inconsistent with previous diagrammatic calculations as well as with

ours. For the Hall effect, our results agree with those of a work [61] in which an independent calculation has been performed. These results were successfully applied for the description of a recent measurement in amorphous Tantalum Nitride films. [20]

The remaining part of this chapter is organized as follows. In Sec. 2.2 we present the basic formalism. We show how the Usadel equation, initially formulated for a given order parameter configuration [85], can be applied to the calculation of fluctuation conductivity. As a next step, in Sec. 2.3 we find a solution of the Usadel equation which allows to determine the order parameter correlation function in the Gaussian approximation. Both ingredients are required for the calculation of the electric current presented in Sec. 2.4. Next, we derive expressions for the longitudinal conductivity that are valid in the entire metallic phase outside the regime of strong fluctuations. Evaluation of the obtained expressions still requires a summation over the Landau levels as well as an integration over slow (bosonic) frequencies, which can be performed analytically only in certain limiting cases. Several such limiting cases are analyzed in detail below, including the region close to T_c and the vicinity of the quantum critical point. By means of a numerical evaluation, we locate the line of the sign change for magnetoresistance $\partial\sigma/\partial B$ and the line $\partial\sigma/\partial T = 0$. We also discuss the existence of a crossing point of the magnetoresistance curves. In Sec. 3.3 we calculate Hall conductivity, generalizing previous calculations [28, 11, 10] to the case of arbitrary temperatures and magnetic fields above the transition.

2.2 Basic equations

In this section we present the equations that form the basis for our calculation of the fluctuation conductivity. After stating the microscopic model, we introduce the Usadel equation that allows to find the quasiclassical Green's function in the

dirty limit, i.e., if the condition $T_c\tau \ll 1$ is fulfilled. Calculation of the conductivity requires knowledge of both the quasiclassical Green's function in the presence of the fluctuating order parameter field and the correlation function of the order parameter field. In the fluctuation regime, which we study here, the order parameter correlation function is governed by the Ginzburg-Landau (GL) action. Fortunately, the GL action can be found from the quasiclassical Green's function itself, i.e., from the solution of the Usadel equation. This procedure will also be described in this section.

We start with the Keldysh action for electrons with short-range BCS-type interaction. After decoupling the interaction with the help of a Hubbard-Stratonovich transformation, the resulting action is split into two parts $S[\Psi, \check{\Delta}] = S_1[\Psi, \check{\Delta}] + S_2[\check{\Delta}]$, where

$$S_1[\Psi, \check{\Delta}] = \int dx \Psi^\dagger(x) [i\hat{\tau}_3\partial_t - \check{H}(x) + \mu + \check{\Delta}(x)] \Psi(x) \quad (2.1)$$

and

$$S_2[\check{\Delta}] = -\frac{2\nu}{\lambda} \int dx \text{tr} [\check{\Delta}^+ \hat{\sigma}_1 \check{\Delta}]. \quad (2.2)$$

Here, ν is the density of states per one spin projection at the Fermi level and μ is the chemical potential. The dimensionless coupling constant in the Cooper channel λ is positive for an attractive interaction. Hereafter, we use the hat symbol as in $\hat{\tau}_3$ to denote 2×2 matrices in Keldysh (K , retarded/advanced) or Gor'kov-Nambu (N , particle/hole) spaces. By $\hat{\sigma}_i$ and $\hat{\tau}_i$ we denote the Pauli matrices in K and N space, correspondingly. The check symbol as in \check{H} denotes 4×4 matrices in the direct product space $K \otimes N$. The trace operation tr in Eq. (2.2) comprises both K and N spaces. The short notation $x = (\mathbf{r}, t)$ is used, and the time integration covers the interval $(-\infty, \infty)$. The single-particle Hamiltonian \check{H} is defined as

$$\check{H} = -\frac{1}{2m} (\nabla - ie\mathbf{A}(\mathbf{r})\hat{\tau}_3)^2 + U(\mathbf{r}) + e\varphi(\mathbf{r}), \quad (2.3)$$

with a static disorder potential U , scalar φ and vector potentials \mathbf{A} , and electron mass m and charge e . In the action, Ψ is a four component vector of Grassmann fields with the following structure:

$$\Psi = \begin{pmatrix} \psi_1 \\ \psi_2 \end{pmatrix}_K, \quad \psi_i = \begin{pmatrix} \chi_{i\uparrow} \\ \chi_{i\downarrow}^* \end{pmatrix}_N \quad (2.4)$$

$$\Psi^\dagger = \left(\psi_1^\dagger, \psi_2^\dagger \right)_K, \quad \psi_i^\dagger = (\chi_{i\uparrow}^*, -\chi_{i\downarrow})_N. \quad (2.5)$$

All terms in the electronic action S_1 are diagonal in K -space except the order parameter field $\check{\Delta} = \hat{\Delta}_0 \hat{\sigma}_0 + \hat{\Delta}_1 \hat{\sigma}_1$, where $\hat{\Delta}_0$ and $\hat{\Delta}_1$ will be referred as classical (cl) and quantum (q) components of the order parameter. These components are non-diagonal in N space: $\hat{\Delta}_i = \Delta_i \hat{\tau}_+ - \Delta_i^* \hat{\tau}_-$, where $\hat{\tau}_\pm = \frac{1}{2}(\hat{\tau}_x \pm i\hat{\tau}_y)$. We arrange the classical and quantum order parameter fields into the vector $\vec{\Delta} = (\Delta_{cl}, \Delta_q)^T$.

The electronic Green's function for the system reads:

$$\check{G}(x, x') = -i \int D\Psi D\check{\Delta} \Psi(x) \Psi^\dagger(x') e^{iS[\Psi, \check{\Delta}]}. \quad (2.6)$$

This expression can be cast in the form

$$\check{G}(x, x') = \int D\vec{\Delta} \check{G}_\Delta(x, x') e^{iS_{GL}[\vec{\Delta}]}, \quad (2.7)$$

where the Ginzburg-Landau action is determined by

$$S_{GL}[\vec{\Delta}] = -i \ln \int D\Psi e^{iS[\Psi, \check{\Delta}]}, \quad (2.8)$$

while

$$\check{G}_\Delta(x, x') = -i \frac{\int D\Psi \Psi(x) \Psi^\dagger(x') e^{iS_1[\Psi, \check{\Delta}]} }{\int D\Psi e^{iS_1[\Psi, \check{\Delta}]} }. \quad (2.9)$$

This Green's function depends on the specific configuration of the order parameter field $\check{\Delta}$.

Physical quantities can be obtained in terms of the disorder-averaged $\langle \check{G}(x, x') \rangle_{dis}$, which can be found as

$$\langle \check{G}(x, x') \rangle_{dis} = \int D\check{\Delta} \langle \check{G}_\Delta(x, x') \rangle_{dis} e^{i\langle S_{GL}[\check{\Delta}] \rangle_{dis}}. \quad (2.10)$$

Here, we average the electronic Green's function separately from the bosonic action. This is a valid approximation for films with dimensionless conductance $g \gg 1$; taking into account cross-correlations between the two terms would give corrections to the Drude conductivity of the order of $1/g^2$, while we are only interested in corrections of the order of $1/g$.

The electric current is related to the Keldysh component of $\langle \check{G}(x, x') \rangle_{dis}$:

$$\mathbf{j} = -\frac{e}{2m} (\nabla_{\mathbf{r}} - \nabla_{\mathbf{r}'}) \langle G^K(x, x') \rangle_{dis, x \rightarrow x'} - \frac{ne^2}{m} \mathbf{A}, \quad (2.11)$$

where n stays for the density of electrons.

In the following, it will be convenient to use the quasiclassical approximation [24, 49, 47]. The quasiclassical Green's function can be introduced as follows. First, one performs the Wigner transform of the disorder-averaged Green's function as

$$\langle \check{G}_\Delta(\mathbf{p}, \mathbf{r}, t_1, t_2) \rangle_{dis} = \int d\boldsymbol{\rho} e^{-i\mathbf{p}\boldsymbol{\rho}} \langle \check{G}_\Delta(x_1, x_2) \rangle_{dis}, \quad (2.12)$$

where $\mathbf{r} = \frac{1}{2}(\mathbf{r}_1 + \mathbf{r}_2)$, $\boldsymbol{\rho} = (\mathbf{r}_1 - \mathbf{r}_2)$. Next, the quasiclassical Green's function is

obtained by integration over the energy variable $\xi = \frac{p^2}{2m} - \mu$ which describes the distance from the Fermi surface:

$$\check{g}_{\mathbf{n}}(\mathbf{r}, t_1, t_2) = \frac{i}{\pi} \int_{-\infty}^{\infty} d\xi \langle \check{G}_{\Delta}(\mathbf{n}(p_F + \xi/v_F), \mathbf{r}, t_1, t_2) \rangle_{dis}. \quad (2.13)$$

In this equation, v_F denotes the Fermi velocity.

In the diffusive limit higher angular harmonics are suppressed and a formulation in terms of the angular-averaged Green's function is possible:

$$\check{g}(\mathbf{r}, t_1, t_2) = \int d\mathbf{n} \check{g}_{\mathbf{n}}(\mathbf{r}, t_1, t_2). \quad (2.14)$$

The function \check{g} satisfies the nonlinear Usadel equation [85, 74]:

$$D\hat{\nabla}(\check{g} \cdot \hat{\nabla}\check{g}) - \{\hat{\tau}_3 \partial_t, \check{g}\} + i[\check{\Delta} - e\check{\varphi}, \check{g}] = 0, \quad (2.15)$$

where the symbol \cdot is used to denote a convolution in time, i.e., integration in the intermediate time variable. The spatial derivative has the following structure: $\hat{\nabla}\check{g} = \nabla\check{g} - ie[\hat{\tau}_3\mathbf{A}, \check{g}]$. An important constraint imposed on the quasiclassical Green's function is that it has to satisfy the normalization condition

$$(\check{g} \cdot \check{g})(t, t') = \check{1}\delta(t - t'). \quad (2.16)$$

In what follows we are interested in Gaussian fluctuations. This means, that the film is considered to be not too close to the superconducting transition. The width of the non-Gaussian region is determined by the Ginzburg number Gi ; in the case of disordered films $Gi \sim g^{-1}$. The precise criterion for the range of validity

of this approximation depends on the quantity in question. Concerning transport phenomena, the non-Gaussian region is wider than for thermodynamics and has been estimated to be of the order of \sqrt{Gi} for the thermal phase transition [51], i.e. it covers the temperature regime for which $|T - T_c| \lesssim \sqrt{Gi}T_c$. To the best of our knowledge, there is no such calculation for the quantum transition (a study of the effect of fluctuations on the critical magnetic field exists [29]). We assume that we are always outside the region of non-Gaussian fluctuations.

Let us now turn to the discussion of the Ginzburg-Landau action. As long as we are interested in Gaussian fluctuations, we need to know $S_{GL}[\vec{\Delta}]$ only up to the second order in $\vec{\Delta}$. Noting the relation

$$\frac{\delta \langle S_{GL}[\vec{\Delta}] \rangle_{dis}}{\delta \Delta_i^*(x_1)} = i \text{tr} [\hat{\sigma}_i \hat{\tau}_- \langle \check{G}_\Delta(x_1, x_1) \rangle_{dis}] - \frac{2\nu}{\lambda} (\hat{\sigma}_1 \vec{\Delta}(x_1))_i, \quad (2.17)$$

we can obtain

$$\langle S_{GL}[\vec{\Delta}] \rangle_{dis} = \int dx_1 dx_2 \vec{\Delta}^\dagger(x_1) \left[-\frac{2\nu}{\lambda} \hat{\sigma}_1 \delta_{x_1, x_2} + \hat{\Pi}(x_1, x_2) \right] \vec{\Delta}(x_2), \quad (2.18)$$

where

$$\hat{\Pi}_{ij}(x_1, x_2) = i \frac{\delta \text{tr} [\hat{\sigma}_i \hat{\tau}_- \langle \check{G}_\Delta(x_1, x_1) \rangle_{dis}]}{\delta \Delta_j(x_2)} \Bigg|_{\vec{\Delta}=0}. \quad (2.19)$$

Importantly, the appearing Green's function at coinciding times and space points is related to the quasiclassical Green's function, and we can write

$$\hat{\Pi}^{ij}(x_1, x_2) = \pi\nu \frac{\delta \text{tr} [\sigma_i \hat{\tau}_- \hat{g}(\mathbf{r}_1, t_1, t_1)]}{\delta \Delta_j(x_2)} \Bigg|_{\vec{\Delta}=0}. \quad (2.20)$$

This result shows that knowledge of the quasiclassical Green's function, i.e., the solution of the Usadel equation, also allows finding the GL action. This observation

considerably simplifies the scheme of calculation of the Gaussian corrections. With the help of the GL action, in turn, one can obtain the order parameter correlation function, which is needed for the calculation of the current.

The charge density and electric current are expressed in terms of the angular-averaged Green's function \check{g} in the following way[74]:

$$\rho(\mathbf{r}, t) = -e\nu \left(2e\phi + \frac{\pi}{2} \text{tr} \langle \hat{\sigma}_1 \hat{g}(\mathbf{r}, t, t) \rangle \right) \quad (2.21)$$

and

$$\mathbf{j}(r, t) = \frac{e\pi\nu D}{2} \text{tr} \langle \hat{\tau}_3 \hat{\sigma}_1 \check{\mathbf{j}}(\mathbf{r}, t, t) \rangle, \quad (2.22)$$

with $\check{\mathbf{j}} = \check{g} \cdot \hat{\nabla} \check{g}$. The angular brackets in this equations symbolize averaging with the action S_{GL} . Relation (2.22) follows from Eq. (2.11) in the diffusion approximation. Aiming for the needed accuracy (the leading order approximation in g^{-1}), it is sufficient to determine $\check{\mathbf{j}}$ up to the second order in the fluctuating field Δ *before* the expansion in the electric field is performed. To see this, let us discuss the quantum components $\hat{g}^{Z,W}$ of the Green's function \hat{g}^R in more detail. We parameterize them as

$$\hat{g}^Z = \begin{pmatrix} z_1 & 0 \\ 0 & z_2 \end{pmatrix}, \quad \hat{g}^W = \begin{pmatrix} w_1 & 0 \\ 0 & w_2 \end{pmatrix} \quad (2.23)$$

and get the following equations:

$$\mathcal{D}^{-1} w_i = I_i^W, \quad \bar{\mathcal{D}}^{-1} z_i = I_i^Z \quad (2.24)$$

with

$$\mathcal{D}^{-1} = D\hat{\nabla}^2 - \partial_{t_1} - \partial_{t_2}, \quad \bar{\mathcal{D}}^{-1} = D\hat{\nabla}^2 + \partial_{t_1} + \partial_{t_2}. \quad (2.25)$$

The collision integrals $I_{1,2}^Z$ are given by

$$\begin{aligned} I_1^Z &= i (\Delta_q \cdot f^* - \bar{f} \cdot \Delta_q^*), \\ I_2^Z &= i (\Delta_q^* \cdot f - \bar{f}^* \cdot \Delta_q) \end{aligned} \quad (2.26)$$

and collision integrals $I_i^W = I_{i,coll}^W - I_{i,neq}^W$ by (this separation is motivated below)

$$\begin{aligned} I_{1,coll}^W &= i(f \cdot J_1 - \bar{J}_1 \cdot \bar{f}^*), \\ I_{2,coll}^W &= i(f^* \cdot J_2 - \bar{J}_2 \cdot \bar{f}), \\ I_{1,neq}^W &= 2j_e \cdot z_1 \cdot j_e + j_e \cdot \bar{f} \cdot \bar{f}^{*'} + f \cdot j_h \cdot \bar{f}^{*'} + \\ &\quad f' \cdot j_h \cdot \bar{f}^* + f' \cdot f^* \cdot j_e, \\ I_{2,neq}^W &= 2j_h \cdot z_2 \cdot j_h + j_h \cdot \bar{f}^* \cdot \bar{f}' + f^* \cdot j_e \cdot \bar{f}' + \\ &\quad f^{*'} \cdot j_e \cdot \bar{f} + f^{*'} \cdot f \cdot j_h. \end{aligned} \quad (2.27)$$

For convenience, we defined ($j_{e,h} = \pm \nabla h_{e,h}$):

$$\begin{aligned} J_1 &= \Delta_q^* - \Delta_c^* \cdot h_e + h_h \cdot \Delta_c^* - h_h \cdot \Delta_q^* \cdot h_e, \\ \bar{J}_1 &= \Delta_q - \Delta_c \cdot h_h + h_e \cdot \Delta_c - h_e \cdot \Delta_q \cdot h_h, \\ J_2 &= \Delta_q - \Delta_c \cdot h_h + h_e \cdot \Delta_c - h_e \cdot \Delta_q \cdot h_h, \\ \bar{J}_2 &= \Delta_q^* - \Delta_c^* \cdot h_e + h_h \cdot \Delta_c^* - h_h \cdot \Delta_q^* \cdot h_e. \end{aligned} \quad (2.28)$$

While $\langle I^Z \rangle = 0$ due to causality[46], the collision integral I^W does not vanish identically after averaging. Nevertheless, its expansion in the electric field can be shown to start from \mathbf{E}^2 . First, we note that $I_{i,neq}^W$ should be related to the production of the heat. Indeed, $\langle I_{i,neq}^W \rangle$ is proportional to the Drude result for the electric current $j_{e,h}$. Next, observe that the terms in $\langle I_{i,neq}^W \rangle$ which are only linear in $j_{e,h}$ are further

multiplied by averages which include the spatial gradients of f and vanish in the absence of an electric field, when the system is isotropic. Hence, $\langle I_{i,neq}^W \rangle = \mathcal{O}(\mathbf{E}^2)$. There is still another term, $I_{i,coll}^W$. For $\mathbf{E} = 0$ it corresponds to the collision integral due to Cooper interactions, which enters the kinetic equation and was calculated by Reizer[68]. Let us just note, that if the only source of non-homogeneity is a spatially varying electric potential (as it is in our case), then the collision integral, written in terms of the gauge invariant particle/hole energies should be independent of the spatial coordinates. As such, it cannot depend on the electric field itself, which is a vector, but only on \mathbf{E}^2 . This is summarized by the equation: $I_{1,2,coll}^W = I_{coll}(\mathbf{E}^2, \epsilon \mp e\phi(x))$. Since for $\mathbf{E} = 0$ it vanishes (provided the electronic distribution function \mathcal{H} is thermal) and depends only on \mathbf{E}^2 , it should be disregarded for the calculations in the linear response.

2.3 Solution of the Usadel equation and the order parameter correlation function

For practical calculations, one needs to resolve the normalization condition (2.16) for the quasiclassical Green's function explicitly. In the framework of a mean-field treatment, one works with the classical order parameter field Δ_{cl} only. In this case ($\Delta_q = 0$) the Green's function can be parameterized as

$$\check{g} = \begin{pmatrix} \hat{g}^R & \hat{g}^K \\ 0 & \hat{g}^A \end{pmatrix}, \quad (2.29)$$

with $\hat{g}^K = \hat{g}^R \cdot \hat{h} - \hat{h} \cdot \hat{g}^A$ and $(\hat{g}^R \cdot \hat{g}^R)_{t,t'} = (\hat{g}^A \cdot \hat{g}^A)_{t,t'} = \hat{1}\delta_{t-t'}$. However, in the presence of the quantum order parameter fluctuation (i.e., for finite Δ_q) this structure is broken and a more general parametrization needs to be considered. In that case, one can generalize (2.29) to take into account fluctuations up to the second order in

Δ :

$$\check{g} = \begin{pmatrix} \hat{g}^R - \hat{h} \cdot \hat{g}^Z & \hat{g}^R \cdot \hat{h} - \hat{h} \cdot \hat{g}^A - \hat{h} \cdot \hat{g}^Z \cdot \hat{h} - \hat{g}^W \\ \hat{g}^Z & \hat{g}^A + \hat{g}^Z \cdot \hat{h} \end{pmatrix}. \quad (2.30)$$

In particular, the lower left corner of this matrix is not equal to zero [92, 46]. This parametrization has the following property:

$$(\hat{g}^R)^2 = (\hat{g}^A)^2 = \hat{1}\delta_{t-t'} + \mathcal{O}(\Delta^4) \quad (2.31)$$

The matrix

$$\hat{h} = \begin{pmatrix} h_e & 0 \\ 0 & h_h \end{pmatrix} \quad (2.32)$$

is called generalized distribution function [47]. Matrices $\hat{g}^{Z,W}$ are diagonal and appear only in the second order in Δ . This holds provided the distribution function \hat{h} satisfies the following normal metal diffusion equation:

$$D\nabla^2\hat{h} - [\partial_t + ie\phi\hat{\tau}_3, \hat{h}] = 0. \quad (2.33)$$

For the purpose of our calculation, we may assume $\hat{g}^Z = \hat{g}^W = 0$. In the case of \hat{g}^Z the reason is the following. For the calculation of the current, the Green's function needs to be inserted into the corresponding expression (2.22) and subsequently averaged over order parameter configurations. There can be two kinds of contributions to the current originating from \hat{g}^Z . First, if it is not combined with any other term arising due to fluctuations, it should be averaged by itself. Since the lower-left corner of the averaged Green's function must equal zero in the Keldysh formalism $\langle \hat{g}^Z \rangle = 0$, contributions of this first type vanish automatically. The second kind of contribution appears when combining \hat{g}^Z with other terms arising due to fluctu-

ations in formula (2.22). Since \hat{g}^Z itself is already quadratic in Δ , this procedure generates contributions to the current which are at least of the fourth order in Δ . These terms are beyond the accuracy of our calculation. The same argument applies to contributions originating from \hat{g}^W , only in this case the average $\langle \hat{g}^W \rangle$ does not vanish identically, but is $\mathcal{O}(\mathbf{E}^2)$.

Therefore, there is no need to keep \hat{g}^W when studying linear response in the electric field. To conclude, for the purpose of our calculation we may work with the simple parametrization given in Eq. 2.29.

In what follows, we consider static and homogeneous electric \mathbf{E} and magnetic \mathbf{B} fields and find it convenient to work in a gauge with time-independent electromagnetic potentials: $\mathbf{E} = -\nabla\phi$ and $\mathbf{B} = \text{curl}\mathbf{A}$ with $\phi = -\mathbf{E}\mathbf{r}$, $\mathbf{A} = (0, Bx, 0)$. Under these conditions and in the absence of superconducting fluctuations, the retarded and advanced sectors of the quasiclassical Green's function are diagonal in N-space and take a particularly simple form

$$\hat{g}^R(t_1, t_2) = -\hat{g}^A(t_1, t_2) = \hat{\tau}_3 \delta_{t_1 - t_2}. \quad (2.34)$$

For a closed system, i.e. in the absence of a connection to an external bath, the distribution function \hat{h} is not yet fixed. Indeed, equation (2.33) has infinitely many solutions. In the presence of interactions, it is convenient to work with the distribution function corresponding to the state of local thermal equilibrium with spatially varying chemical potential:

$$\hat{h} = \begin{pmatrix} h_e & 0 \\ 0 & h_h \end{pmatrix}, \quad h_{e,h} = \mathcal{H}(\epsilon \mp e\phi(x)) \quad (2.35)$$

where

$$\mathcal{H}(\epsilon) = \tanh \frac{\epsilon}{2T}. \quad (2.36)$$

This particular choice is especially convenient for linear response studies, because deviations of $\langle \hat{g}^W \rangle$ from zero which arise due to interactions are pushed to the second order in the electric field. This considerably simplifies perturbation theory. Note that temperature is still arbitrary and is determined by the heat balance with a substrate or with contacts. Meanwhile, by neglecting $\langle \hat{g}^W \rangle$ we dismiss the heating effect of the electric field.

In the presence of superconducting fluctuations, the quasiclassical Green's function acquires off-diagonal components in N -space. For the analysis of the Gaussian fluctuation regime, the deviations from the simple form given in Eq. 2.34 are small and may be treated as a perturbation. With this in mind, we resolve the remaining constraints (2.31) as:

$$\hat{g}^R = \begin{pmatrix} 1 - \frac{1}{2} f \cdot f^* & f \\ f^* & -1 + \frac{1}{2} f^* \cdot f \end{pmatrix}, \quad (2.37)$$

$$\hat{g}^A = \begin{pmatrix} -1 + \frac{1}{2} \bar{f} \cdot \bar{f}^* & -\bar{f} \\ -\bar{f}^* & 1 - \frac{1}{2} \bar{f}^* \cdot \bar{f} \end{pmatrix}, \quad (2.38)$$

From the solution of the Usadel equation it will follow that f, \bar{f} etc. are $\mathcal{O}(\Delta)$. The functions f and f^* as well as \bar{f} and \bar{f}^* are considered as independent: they become complex conjugates of each other only when Δ_q is neglected.

We introduce parametrization (2.30) into Eq. (2.15) and neglect terms of the

third order in Δ . As a result, we find for f the equation $\mathcal{C}^{-1}f = V$, where the operator \mathcal{C}^{-1} is given by

$$\mathcal{C}^{-1} = D\hat{\nabla}^2 - \partial_{t_1} + \partial_{t_2} \quad (2.39)$$

and the gauge invariant derivative is: $\hat{\nabla}f = (\nabla - 2ie\mathbf{A})f$. As one may notice, this equation describes the response of the field f to the order parameter Δ , which enters this equation in the following combination:

$$V_{t_1, t_2}(\mathbf{r}) = 2i [\Delta_{cl}(\mathbf{r}, t_1) \delta_{t_1 - t_2} + h_e(\mathbf{r}, t_1 - t_2) \Delta_q(\mathbf{r}, t_2)]. \quad (2.40)$$

Similar equations arise for f^* , \bar{f} , and \bar{f}^* with appropriately modified differential operators and functions V^* , \bar{V} and \bar{V}^* . Taking into account the explicit form of $h_{e,h}$ one may conclude that $\bar{f}_{t_1, t_2} = -f_{t_2, t_1}$ (the same property holds for f^*). Note that a static electric potential does not enter the equation for f . This is one of the advantages of the gauge in which the electric field is expressed through the scalar potential.

The equation for f can easily be solved after a Fourier transformation to the frequency domain according to

$$f(t_1, t_2) = \int f(\epsilon_1, \epsilon_2) e^{-i(\epsilon_1 t_1 - \epsilon_2 t_2)} (d\epsilon_1) (d\epsilon_2). \quad (2.41)$$

Here we used notation $(d\epsilon) = d\epsilon/2\pi$. To proceed further, we pass to the Landau level (LL) basis with eigenfunctions $\psi_{np}(\mathbf{r})$ of the kinetic energy operator

$$-D(\nabla - 2ie\mathbf{A})^2 \psi_{np}(\mathbf{r}) = \epsilon_n \psi_{np}(\mathbf{r}). \quad (2.42)$$

This equation describes a "particle" with a mass equal to $1/2D$. We choose to work in the Landau gauge, for which the eigenfunctions ψ_{np} are numbered by the momentum p and LL number n :

$$\psi_{np}(\mathbf{r}) = e^{ipy} \chi_n(x - pl_B^2) \quad (2.43)$$

with magnetic length $l_B = 1/\sqrt{2|e|B}$ (for a "particle" with charge $2|e|$) and

$$\chi_n(x) = \frac{1}{\sqrt{l_B}} \frac{e^{-x^2/2l_B^2}}{\pi^{1/4} \sqrt{2^n n!}} H_n(x/l_B). \quad (2.44)$$

Note that a description based on the Usadel equation is valid as long as we consider the regime of classically weak magnetic fields, for which $\omega_c = \frac{|e|B}{m}$ satisfies $\omega_c \tau \ll 1$. This means that the quantization of the orbital motion of the quasiparticles can be neglected. In contrast, the LL quantization of the collective modes and Cooperons $\epsilon_n = \Omega_c (\frac{1}{2} + n)$ with $\Omega_c = 4|e|DB$ may still be important in the region of magnetic fields and temperatures we are interested in.

The solution for f is conveniently written in terms of the Cooperon propagator, which is diagonal in the chosen basis: $\langle n, p | \mathcal{C} | m, p \rangle = \delta_{mn} C_n(\epsilon_1 + \epsilon_2)$ with

$$C_n(\epsilon) = (i\epsilon - \epsilon_n - \tau_\phi^{-1})^{-1}. \quad (2.45)$$

Here, we introduced the dephasing time τ_ϕ . The role of τ_ϕ is to provide the long-time decay of the Cooperon, which is necessary to render corrections due to single-particle interference processes finite. These processes include weak localization and the anomalous Maki-Thompson correction (an analog of weak antilocalization) that diverge in the absence of a magnetic field for $\tau_\phi^{-1} = 0$. Dephasing can be provided by

magnetic impurities or inelastic processes, i.e. electron-electron or electron-phonon collisions. For low temperatures, electron-electron collisions dominate. Outside the region of strong fluctuations (i.e., in the Gaussian regime), one can consider the dephasing rate as energy independent and equal to the sum of rates due to the Coulomb[8] and Cooper channels[50, 18]. In our study, we do not specify the dominant dephasing mechanism relevant for τ_ϕ and consider it as an independent parameter.

The solution of the equation $\mathcal{C}^{-1}f = V$ for f reads:

$$f_{np}(\epsilon_1, \epsilon_2) = C_n(2\epsilon) \int V_{\epsilon_1, \epsilon_2}(\mathbf{r}') \psi_{np}^*(\mathbf{r}') d\mathbf{r}', \quad (2.46)$$

where

$$V_{\epsilon_1, \epsilon_2}(\mathbf{r}) = 2i [\Delta_d(\mathbf{r}, \omega) + h_e(\mathbf{r}, \epsilon + \omega/2) \Delta_q(\mathbf{r}, \omega)] \quad (2.47)$$

with shorthand notation $\epsilon = (\epsilon_1 + \epsilon_2)/2$ and $\omega = \epsilon_1 - \epsilon_2$. Analogous equations hold for f^* , \bar{f} and \bar{f}^* .

Having found approximate solutions for \hat{g}^R and \hat{g}^A , we turn to the *GL* action S_{GL} . As follows from Eq. 2.18 in combination with Eq. 2.20, it is sufficient to know $\hat{g}^{R(A)}$ at the first order in Δ to determine S_{GL} in the Gaussian approximation. We write the GL action in the form:

$$S_{GL}[\vec{\Delta}] = \int \text{tr} \left(2\nu \vec{\Delta}^+(-\omega, \mathbf{r}) \mathcal{L}^{-1}(\omega, \mathbf{r}, \mathbf{r}') \vec{\Delta}(\omega, \mathbf{r}') \right) \quad (2.48)$$

with

$$\mathcal{L}^{-1} = \begin{pmatrix} 0 & \mathcal{L}_{12}^{-1} \\ \mathcal{L}_{21}^{-1} & \mathcal{L}_{22}^{-1} \end{pmatrix}. \quad (2.49)$$

Arguments $(\omega, \mathbf{r}, \mathbf{r}')$ of \mathcal{L}^{-1} are omitted in what follows.

A straightforward calculation according to Eq. (2.18) gives:

$$\mathcal{L}_{21}^{-1} = \sum_{np} \psi_{np}(\mathbf{r}) \psi_{np}^*(\mathbf{r}') \left[\int \frac{\mathcal{H}_{\epsilon - \omega/2 + e\phi(\mathbf{r})} d\epsilon}{2\epsilon + i(\epsilon_n + \tau_\phi^{-1})} - \frac{1}{\lambda} \right]. \quad (2.50)$$

The rest of the elements of \mathcal{L}^{-1} are related to this one according to $\mathcal{L}_{12}^{-1} = (\mathcal{L}_{21}^{-1})^+$ and

$$\mathcal{L}_{22}^{-1} = \mathcal{B}(\omega - e\phi(\mathbf{r}) - e\phi(\mathbf{r}')) [\mathcal{L}_{21}^{-1} - \mathcal{L}_{12}^{-1}], \quad (2.51)$$

where the bosonic distribution function is defined as

$$\mathcal{B}(\omega) = \coth(\omega/2T). \quad (2.52)$$

One can see, that the components of \mathcal{L}^{-1} are not independent. Just as the components of \mathcal{L} , they are related by the generalized fluctuation-dissipation theorem, see Eq. (2.51), valid in the quasi-equilibrium state. Thus, only \mathcal{L}_{21}^{-1} needs to be calculated explicitly. The evaluation of the ϵ integral in Eq. (2.50) is straightforward and yields:

$$\mathcal{L}_{21}^{-1} = \sum_{np} \psi_{np}(\mathbf{r}) \psi_{np}^*(\mathbf{r}') \mathcal{E}_n(\omega - 2e\phi(\mathbf{r})), \quad (2.53)$$

where

$$\mathcal{E}_n(\omega) = \ln \frac{T_c}{T} + \psi\left(\frac{1}{2}\right) - \psi^R(n, \omega) \quad (2.54)$$

and

$$\psi^{R(A)}(n, \omega) = \psi\left(\frac{1}{2} + \frac{\epsilon_n + \tau_\phi^{-1} \mp i\omega}{4\pi T}\right). \quad (2.55)$$

We have introduced the BCS transition temperature $T_c = \frac{2\gamma\omega_D}{\pi} \exp(-\frac{1}{\lambda})$, where ω_D is the Debye frequency and $\gamma \approx 1.78$. The symbol ψ stands for the Digamma

function[3]. In deriving asymptotic expressions, we will use the following properties of this function: $\psi'(1/2) = \pi^2/2$ and $\psi(x) \approx \ln x$ for $x \gg 1$.

The line of the superconducting transition on the mean field level is determined by the equation $\mathcal{E}_{n=0}(\omega = 0) = 0$. In the absence of dephasing $\tau_\phi = \infty$ this gives for the upper critical field

$$B_c(T = 0) = \frac{\pi T_c}{2\gamma D}. \quad (2.56)$$

Let us discuss the effect of dephasing on the transition line. Since the fluctuation propagator depends on the dephasing rate, the transition temperature is shifted due to τ_ϕ . Furthermore, since τ_ϕ depends on the magnetic field as well as on the temperature, the presence of τ_ϕ in the fluctuation propagator changes the shape of the transition line as a whole. Dephasing also affects the magnetoconductivity. This effect has been taken into account in the analysis of the experimental data on magnetoconductivity of thin superconducting InO films[19].

As can be seen from the right-hand side of Eq. (2.53), \mathcal{L}_{21}^{-1} is not translation invariant. However, by splitting off a gauge-dependent factor it can be rewritten in the following form:

$$\mathcal{L}_{21}^{-1}(t, \mathbf{r}, \mathbf{r}') = e^{-iS_g(t, \mathbf{r}, \mathbf{r}')} \bar{\mathcal{L}}_{21}^{-1}(t, \mathbf{r} - \mathbf{r}'), \quad (2.57)$$

where S_g is defined as

$$S_g(t, \mathbf{r}, \mathbf{r}') = e(\phi(\mathbf{r}) + \phi(\mathbf{r}'))t - e(\mathbf{A}(\mathbf{r}) + \mathbf{A}(\mathbf{r}'))(\mathbf{r} - \mathbf{r}') \quad (2.58)$$

and $\bar{\mathcal{L}}_{21}^{-1}$ is translational and gauge invariant. We nevertheless prefer to work with the operator \mathcal{L}^{-1} in its original form.

In order to find the order parameter correlation functions, one has to invert the operator \mathcal{L}^{-1} given by Eq. (2.49) with the following result:

$$\mathcal{L} = \begin{pmatrix} \mathcal{L}^K & \mathcal{L}^R \\ \mathcal{L}^A & 0 \end{pmatrix}, \quad (2.59)$$

where

$$\mathcal{L}^R = (\mathcal{L}_{21}^{-1})^{-1}, \quad \mathcal{L}^A = (\mathcal{L}_{12}^{-1})^{-1}, \quad \mathcal{L}^K = -\mathcal{L}^R \mathcal{L}_{22}^{-1} \mathcal{L}^A. \quad (2.60)$$

The order parameter correlation functions are given by:

$$\begin{aligned} \langle \Delta_{cl}(\omega) \Delta_c^*(-\omega) \rangle &= \frac{i}{2\nu} \mathcal{L}^K, \\ \langle \Delta_{cl}(\omega) \Delta_q^*(-\omega) \rangle &= \frac{i}{2\nu} \mathcal{L}^R, \\ \langle \Delta_q(\omega) \Delta_{cl}^*(-\omega) \rangle &= \frac{i}{2\nu} \mathcal{L}^A, \\ \langle \Delta_q(\omega) \Delta_q^*(-\omega) \rangle &= 0. \end{aligned} \quad (2.61)$$

In equilibrium, $\mathcal{L}_{E \rightarrow 0}^{R(A)}(\omega) \equiv L^{R(A)}(\omega)$ is diagonal in the LL basis, and reads as follows

$$L_n^R(\omega) = \mathcal{E}_n^{-1}(\omega). \quad (2.62)$$

For the Keldysh propagator this gives, according to Eq. (2.60):

$$\mathcal{L}_{E \rightarrow 0}^K(\omega) = \mathcal{B}(\omega) (L^R(\omega) - L^A(\omega)) \equiv L^K(\omega). \quad (2.63)$$

While we have already neglected the heating induced by the electric field, we still keep other nonlinear effects. For example, one may consider the decay of fluctuating Cooper pairs due to the acceleration of the paired electrons caused by the electric

field. It was considered before on the basis of the phenomenological theory[70, 34, 88, 62] (with only AL process included). At $T \sim T_c$ this effect becomes essential at electric fields of the order of $E \sim T_c/e\xi_{GL}$ that can be rather small due to the divergence of the coherence length ξ_{GL} at the transition.

In the following calculations all nonlinear effects will be neglected. In the linear response regime, we need to find propagators at first order in the electric field. Concerning the dependence of \mathcal{L} on spatial arguments, we will consider it as an operator in the basis of the LLs, the same is assumed regarding the position operator \mathbf{r} . Hence, in the equations below these two operators do not commute. We linearize \mathcal{L}_{21}^{-1} , looking for the first order correction to its equilibrium value. In the equations below we do not indicate the frequency dependence of propagators, having in mind that all functions have the argument ω . Taking into account first-order corrections in the electric field we write

$$\mathcal{L}_{21}^{-1} = (1 + 2e\mathbf{E}\mathbf{r}\partial_\omega)\mathcal{E}. \quad (2.64)$$

For \mathcal{L}^R this gives:

$$\mathcal{L}^R = L^R + \delta L^R, \quad (2.65)$$

$$\delta L^R = -2e\mathbf{E}L^R\mathbf{r}\partial_\omega\mathcal{E}L^R \quad (2.66)$$

and \mathcal{L}^A can be found by hermitian conjugation. Let us turn to \mathcal{L}^K . In order to find it, we need \mathcal{L}_{22}^{-1} given by Eq. (2.51):

$$\mathcal{L}_{22}^{-1} = \mathcal{B}(\mathcal{L}_{21}^{-1} - \mathcal{L}_{12}^{-1}) + e\mathbf{E}\partial_\omega\mathcal{B}\{(\mathcal{E} - \mathcal{E}^*), \mathbf{r}\}, \quad (2.67)$$

where curly brackets denote an anticommutator. Plugging this expression into

Eq. (2.60), we obtain

$$\mathcal{L}^K = L^K + \delta L^K \quad (2.68)$$

and

$$\delta L^K = \mathcal{B}(\delta L^R - \delta L^A) - e\mathbf{E}\partial_\omega \mathcal{B}L^R\{(\mathcal{E} - \mathcal{E}^*), \mathbf{r}\}L^A. \quad (2.69)$$

Now, the order parameter correlation functions given by Eqs. (2.61) are fully specified, and we can proceed to the calculation of the electric current.

To summarize, we have collected the basic elements of the formalism used for the calculation of the fluctuation conductivity. Once the quasiclassical Green's function is found as a solution of the Usadel equation (2.15), the current can be obtained from Eq. (2.22). Since the quasiclassical Green's function is a functional of the order parameter configuration, formula (2.22) for the current includes an average with respect to the GL action. This action, in turn, can be found from the quasiclassical Green's function via Eqs. (2.18) and (2.20) and thus a closed scheme is established. As we have already argued, it will be sufficient for our purposes to work with \hat{g} given by Eq. (2.29) where $\hat{g}^{R(A)}$ are defined in Eqs. (2.37), (2.38), and the distribution function \hat{h} presented in Eq. (2.35).

2.4 Fluctuation corrections: derivation

Before studying the fluctuation corrections, we first show how to obtain Drude conductivity from the formalism. Input are the normal-metal solution of the Usadel equation: $\hat{g}^R = -\hat{g}^A = \hat{\tau}_3$ and the distribution function in the presence of the electric field, Eq. (2.35). This gives, according to Eq. (2.22), the electric current:

$$\mathbf{j}^{(n)} = e\pi\nu D \text{tr} \hat{\tau}_3 \nabla \hat{h} = 2\nu e^2 D \mathbf{E}. \quad (2.70)$$

This results in the Drude formula $\sigma_D = 2\nu e^2 D$.

Now we turn to the calculation of the fluctuation corrections. Starting with expression (2.22), we substitute for \hat{g} the parametrization (2.29) and obtain the following contributions to the current

$$\mathbf{j} = \mathbf{j}^{(n)} + \mathbf{j}^{(dos)} + \mathbf{j}^{(an)} + \mathbf{j}^{(sc)}. \quad (2.71)$$

Here, all terms besides $\mathbf{j}^{(n)}$ depend on the realization of the superconducting order parameter Δ and have to be averaged using the order parameter correlation functions (2.61). The fluctuation contributions can be written in the following form (hereafter the derivative is with respect to the energy argument):

$$\mathbf{j}^{(dos)} = 2\pi e^2 D \mathbf{E} \int \mathcal{H}'(\epsilon) \delta\nu(\epsilon) (d\epsilon), \quad (2.72)$$

$$\mathbf{j}^{(an)} = 2\pi e^2 D \mathbf{E} \int \mathcal{H}'(\epsilon) \vartheta(\epsilon) (d\epsilon), \quad (2.73)$$

$$\mathbf{j}^{(sc)} = 2\pi e D \int \mathcal{H}(\epsilon) \mathbf{j}^{(s)}(\epsilon) (d\epsilon). \quad (2.74)$$

The quantities which appear in these expressions are defined as follows

$$\delta\nu(\epsilon) = -\frac{\nu}{8} \langle f \cdot f^* + f^* \cdot f + (f \leftrightarrow \bar{f}) \rangle_{\epsilon, \epsilon}, \quad (2.75)$$

$$\vartheta(\epsilon) = -\frac{\nu}{4} \langle \bar{f} \cdot f^* + \bar{f}^* \cdot f \rangle_{\epsilon, \epsilon}, \quad (2.76)$$

and

$$j_{\alpha}^{(s)}(\epsilon) = \frac{\nu}{8} \left\langle f \cdot \hat{\nabla}_{\alpha} f^* - \hat{\nabla}_{\alpha} f \cdot f^* - (f \leftrightarrow \bar{f}) - (f \leftrightarrow f^*) \right\rangle_{\epsilon, \epsilon}. \quad (2.77)$$

The rationale behind this decomposition is the following: (i) The function $\delta\nu(\epsilon)$ describes the correction to the electronic density of states, see $\delta\nu(\epsilon)$ in Eq. (2.78) below. (ii) The $\vartheta(\epsilon)$ -term has a peculiar analytic structure. Indeed, it contains

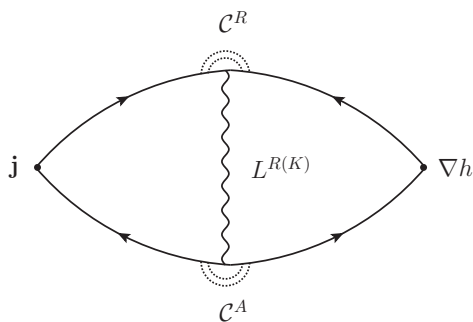


Figure 2.1: Anomalous Maki-Thompson diagram

a convolution of f^* and \bar{f} , which upon averaging gives rise to a product of two Cooperons of different analytical structure, \mathcal{C}^R and \mathcal{C}^A , and the imaginary part of the fluctuation propagator, $\text{Im}L^R$. This allows to identify this term with the anomalous Maki-Thompson contribution. For an illustration of this point, we refer to Fig. 2.1.

(iii) The $j_\alpha^{(s)}$ -term can be interpreted as the fluctuating supercurrent density. This term is the result of the expansion in the electric field of the fermionic distribution function h_e entering either the combination V (see Eq. (2.40)) or the order parameter correlation function \mathcal{L} (see Eqs. (2.66) and (2.69)). The former contribution is purely quantum, while the latter comprises both quantum and classical parts, which are of different importance in the different regions of the phase diagram.

We note that the decomposition (i) - (iii) is very different from the conventional classification based on the diagrams in the Matsubara technique. The difference is related to two main points: a) in the traditional technique a response to a time-dependent vector potential is calculated and b) in the present method there is no need for an analytic continuation.

It is obvious from Eqs. (2.72) and (2.73) that $\mathbf{j}^{(dos)}$ and $\mathbf{j}^{(an)}$ contribute only to the longitudinal current, while $\mathbf{j}^{(sc)}$ contributes to the transverse current as well. In this context it should be kept in mind that in the Usadel equation, which was used

as a starting point for our calculation, the Lorentz force acting on the quasiparticle was neglected.

To proceed further, we substitute the expressions for f , f^* , \bar{f} and \bar{f}^* in the LL basis (cf. Eq. (2.46)) into the expressions above and average them with respect to order parameter fluctuations. The quantities $\delta\nu(\epsilon)$ and $\vartheta(\epsilon)$ are equilibrium properties of the system and are independent of the electric field, and that is why their calculation is relatively simple. Let us start with the DOS correction which can be understood as a renormalization of the quasiparticle density-of-states:

$$\delta\nu(\epsilon) = v \sum_n \text{Im} \int (d\omega) C_n^2 (2\epsilon - \omega) [L_n^K(\omega) + L_n^R(\omega) \mathcal{H}(\epsilon - \omega)]. \quad (2.78)$$

Here, $v = 1/2\pi l_B^2$ is the number of states per unit area of a LL. This factor appears with each summation over LLs. In the continuous limit $v \sum_n \rightarrow \sum_q$ and the above expression becomes identical to the one in Eq. (372) in the review by Kamenev and Levchenko[46]. Note that $\int \delta\nu(\epsilon) d\epsilon = 0$. This is because the interaction cannot change the total number of single-particle states, but just redistributes them.

Turning to the anomalous MT correction, we find that it is due to a real process. Indeed, $\vartheta(\epsilon)$ can be presented in the following form:

$$\vartheta(\epsilon) = v \sum_n \frac{\tau_{out,n}^{-1}(\epsilon)}{\epsilon_n + \tau_\phi^{-1}}, \quad (2.79)$$

where $\tau_{out,n}^{-1}$ is the partial (n) out-scattering rate for quasiparticles arising due to the decay of superconducting fluctuations[68]:

$$\tau_{out,n}^{-1}(\epsilon) = 2 \int (d\omega) \text{Re} C_n (2\epsilon - \omega) \text{Im} L_n^R(\omega) [\mathcal{B}(\omega) + \mathcal{H}(\epsilon - \omega)]. \quad (2.80)$$

The discussed correction disappears at zero temperature. This makes it essentially different from the DOS correction which exists down to zero temperature. The sign of the anomalous MT correction is always positive. It is closely related to weak antilocalization, and can be interpreted as an interference effect in the singlet Cooper channel, enhanced by coherent scattering on the fluctuating order parameter.

Next, we turn to the calculation of the supercurrent $\mathbf{j}^{(s)}$, which is more complicated because non-equilibrium terms in the fluctuation propagators have to be taken into account. The calculation gives:

$$j_x^{(s)}(\epsilon) = \frac{eE_x}{8}v \sum_n \int (d\omega)(n+1) \{A_{n,n+1}(\omega, \epsilon)\}_- \quad (2.81)$$

and

$$j_y^{(s)}(\epsilon) = \frac{eE_x}{8}v \sum_n \int (d\omega)i(n+1) \{A_{n,n+1}(\omega, \epsilon) - A_{n,n}(\omega, \epsilon)\}_+. \quad (2.82)$$

In these equations, the notation $\{X\}_\pm = X \pm \tilde{X}$ is introduced, where \tilde{X} is obtained from X by the substitution $n \leftrightarrow n+1$. Let us comment more on the details of the calculation.

We start with expression (2.77). After substituting the solution for f and averaging in Δ we get:

$$j_\alpha^{(s)}(\epsilon) = \frac{1}{8}eE \sum_{mn} \int (d\omega) I_{\alpha,mn} A_{mn}(\omega, \epsilon) \quad (2.83)$$

Here $I_{\alpha,mn}$ represents the result of integration in the momentum quantum number:

$$I_{\alpha,mn} = 2i \int (dp) \text{Im} \left(\psi_{mp}(\mathbf{r}) \hat{\nabla}_\alpha \psi_{np}^*(\mathbf{r}) \right) \langle np | x | mp \rangle \quad (2.84)$$

and $A_{mn} = \sum_k A_{mn}^{(k)}$ has several contributions, which arise from different ways to expand propagators or bosonic/fermionic distribution functions in the electric field. The next step is to calculate integral (2.84): taking into account $\langle n, p | x | m, p \rangle = x_{nm} + pl_B^2 \delta_{nm}$, where x_{nm} are matrix elements, calculated with $\chi_n(x)$, we obtain:

$$I_x(m, n) = 2vx_{nm}\partial_{mn}, \quad (2.85)$$

$$I_y(m, n) = \frac{2i}{l_B^2}v(x_{nm}x_{mn} - \delta_{mn}(x^2)_{mn}). \quad (2.86)$$

We also take into account:

$$x_{mn} = \frac{l_B}{\sqrt{2}}(\sqrt{n+1}\delta_{m,n+1} + \sqrt{n}\delta_{m,n-1}) \quad (2.87)$$

$$\partial_{mn} = -\frac{1}{\sqrt{2}l_B}(\sqrt{n+1}\delta_{m,n+1} - \sqrt{n}\delta_{m,n-1}) \quad (2.88)$$

and obtain the result, presented in (2.81), (2.82).

The next step is to substitute $\delta\nu(\epsilon)$, $\vartheta(\epsilon)$ and $j_\alpha^{(s)}(\epsilon)$ into the expressions (2.72)-(2.74) and to perform the integration in ϵ . The results of these integrations can be expressed in terms of \mathcal{E}_n :

$$\delta\sigma_{\parallel}^{(dos)} = -2e^2 Dv \sum_n \int (d\omega) \left[\mathcal{B} \text{Im} \frac{\mathcal{E}_n''}{\mathcal{E}_n} + \mathcal{B}' \frac{\text{Im} \mathcal{E}_n \text{Re} \mathcal{E}_n'}{|\mathcal{E}_n|^2} \right], \quad (2.89)$$

$$\delta\sigma_{\parallel}^{(an)} = -4e^2 Dv \sum_n \int (d\omega) \mathcal{B}' \frac{\text{Im}^2 \mathcal{E}_n}{|\mathcal{E}_n|^2} \frac{1}{\tau_\phi^{-1} + \epsilon_n}, \quad (2.90)$$

$$\delta\sigma_i^{(sc)} = -2e^2 D\Omega_c^{-1}v \sum_n \int (d\omega) (n+1) (\mathcal{B}u_i + \mathcal{B}'v_i), \quad (2.91)$$

where $i = \parallel, \perp$. For the longitudinal (\parallel) conductivity,

$$u_{\parallel} = \text{Re} [K_n K'_n L_n^R L_{n+1}^R] \quad (2.92)$$

and

$$v_{\parallel} = 2\text{Re} K_n \text{Im} [\mathcal{E}_n + \mathcal{E}_{n+1}] \text{Im} [L_n^R L_{n+1}^A] + \text{Im} K_n \text{Im} [L_{n+1}^R - L_n^R] \quad (2.93)$$

with $K_n(\omega) = \psi_{n+1}^R(\omega) - \psi_n^R(\omega)$. For the transversal (\perp) conductivity (assuming negatively charged carriers $e < 0$ for the rest of the text; otherwise, the sign of the Hall conductivity should be reversed), we obtain:

$$u_{\perp} = 2\text{Im} [K_n L_n^R L_{n+1}^R (\mathcal{E}'_n + \mathcal{E}'_{n+1})] - 2\Omega_c \text{Re} \left\{ (L_n^R)^2 \mathcal{E}'_n \psi_n^{R'} \right\}_+ - \quad (2.94)$$

$$-\text{Im} [K'_n (L_{n+1}^R + L_n^R)] + \Omega_c \text{Re} \left\{ \psi_n^{R'} L_n^R \right\}_+,$$

and

$$v_{\perp} = -2\text{Im}(\psi_n^R + \psi_{n+1}^R) \text{Re} K_n \text{Re} [L_n^R L_{n+1}^A] - 2\Omega_c \left\{ \text{Im} \psi_n^R \text{Im} \psi_n^{R'} L_n^R L_n^A \right\}_+ - \quad (2.95)$$

$$-\text{Im} K_n \text{Re} (L_{n+1}^R + L_n^R) + \Omega_c \text{Re} \left\{ L_n^R \text{Re} \psi_n^{R'} \right\}_+.$$

To conclude, we have derived fluctuation conductivity due to electron-electron interactions in the Cooper channel in the Gaussian approximation. Equations (2.89)-(2.91) describe the contribution of superconducting fluctuations to the conductivity everywhere in the (B, T) phase diagram (outside the regime of strong fluctuations close to the transition). In the rest of the chapter we discuss different limiting cases and elaborate on asymptotics of these general formulas.

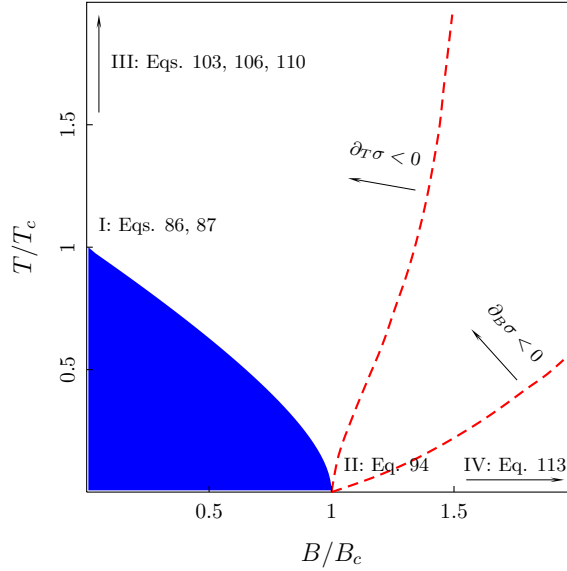


Figure 2.2: Phase Diagram for the correction to the longitudinal conductivity $\delta\sigma_{xx}$. The corresponding equations are written in the text.

2.5 Discussion of the results for longitudinal conductivity

At the end of the previous section, we provided general formulas for the fluctuation corrections to conductivity. In certain asymptotic regions of the phase diagram they are amenable to an analytic treatment. Following this route, we are able to compare our results to the previous studies. The derived formulas can also be subjected to a numerical analysis, which allows to find the corrections in the entire normal part of the phase diagram.

We will discuss the following asymptotic regions in the phase diagram: The vicinities of the classical (I) and quantum (II) transition points, the region of high temperatures and small magnetic fields (III) and the region of high magnetic fields and low temperatures (IV). The corresponding regions are indicated on the phase

diagram displayed in Fig. 2.2. By means of a numerical evaluation, we locate the line which describes the transition from positive to negative magnetoresistance ($\partial_B \sigma = 0$), and the line which characterizes the change of the temperature dependence of the total correction $\partial_T \sigma = 0$.

2.5.1 GL region (I)

In this region, $\delta\sigma_{\parallel}^{(sc)}$ and $\delta\sigma_{\parallel}^{(an)}$ are the most important. Since the leading contribution comes from small bosonic momenta and frequencies ($\omega, Dq^2 \lesssim T - T_c$), in order to extract the result, one should expand the equilibrium propagator in ω/T and ϵ_n/T :

$$[L_n^{R(A)}(\omega)]^{-1} \approx \frac{\pi}{8T} [-\tau_{GL}^{-1} - \epsilon_n \pm i\omega], \quad (2.96)$$

where

$$\tau_{GL} = \frac{\pi}{8T \ln T/T_c}. \quad (2.97)$$

In this section we assume $\tau_{\phi} \gg \tau_{GL}$ and neglect τ_{ϕ} in the fluctuation propagator. Substituting the expression for the propagators $L_n^{R(A)}$ to Eqs. (2.90) and (2.91), integrating in frequency (only the term proportional to \mathcal{B}' contributes), and performing the summation over the LL index, we obtain:

$$\delta\sigma_{\parallel}^{(an)} = \frac{e^2}{\pi} T \tau_{GL} \left[\psi\left(\frac{1}{2} + s\right) - \psi\left(\frac{1}{2} + s \frac{\tau_{GL}}{\tau_{\phi}}\right) \right] \quad (2.98)$$

and

$$\delta\sigma_{\parallel}^{(sc)} = \frac{2e^2}{\pi} (T \tau_{GL}) s \left[-1 - 2s\psi(s) + 2s\psi\left(\frac{1}{2} + s\right) \right], \quad (2.99)$$

with

$$s = (\Omega_c \tau_{GL})^{-1}. \quad (2.100)$$

These results are in agreement with existing calculations. In particular, $\delta\sigma_{\parallel}^{(sc)}$ was obtained phenomenologically by Abrahams et al.[1], and the Maki-Thompson contribution was discussed for finite magnetic fields in Ref. [40]. Note, that the parameter s divides the region (I) into two parts with a distinct behavior. The zero-field limit is recovered for $s \gg 1$:

$$\delta\sigma_{\parallel}^{(an)} = \frac{e^2}{\pi} T\tau_{GL} \ln(\tau_{\phi}/\tau_{GL}), \quad \delta\sigma_{\parallel}^{(sc)} = \frac{e^2}{2\pi} T\tau_{GL}. \quad (2.101)$$

In the absence of a magnetic field, the importance of the anomalous MT correction, $\delta\sigma_{\parallel}^{(an)}$, in comparison with $\delta\sigma_{\parallel}^{(sc)}$ is determined by the ratio τ_{ϕ}/τ_{GL} . Indeed, the MT term diverges in the absence of dephasing, $\tau_{\phi} \rightarrow \infty$, and becomes comparable to the AL correction when $\tau_{\phi} \sim \tau_{GL}$. As the ratio decreases further, the relative importance of the MT correction diminishes.

For completeness, let us discuss the DOS correction in region (I). In the vicinity of the critical temperature, $\delta\sigma_{\parallel}^{(dos)}$ is weakly (only logarithmically) singular. The reason is that interactions preserve the total density of states, and the integration with \mathcal{H}' in Eq. (2.72) is (comparatively) wide: $\epsilon \lesssim T \approx T_c$. For zero magnetic field one gets:

$$\delta\sigma_{\parallel}^{(dos)} = -\frac{7\zeta(3)e^2}{\pi^4} \ln T\tau_{GL}. \quad (2.102)$$

A contribution of the same form originates also from the anomalous MT correction as a subleading term, with a numerical coefficient -14 instead of -7 . It is instructive to perform a comparison with the previously known result in this region. For that, one should sum all terms of the kind $\delta\sigma = c\frac{\zeta(3)}{\pi^4} \ln T\tau_{GL}$. In the diagrammatic calculation,[22] one obtains the coefficient $c = -14$ as the combined contribution of all diagrams with a horizontal interaction line. Those diagrams taken together

are often referred to as the DOS-type corrections. In addition, regular MT, AL and anomalous MT diagrams come with the coefficients $c = -7$, $c = 14$ and $c = -14$, correspondingly. One can see that only after summation of all logarithmic terms of this kind, the results of the two approaches coincide, and one obtains in both cases a total numerical coefficient $c_{tot} = -21$.

We would like to stress that according to Eq. (2.72) it is the contribution $\delta\sigma_{\parallel}^{(dos)}$ rather than the sum of all horizontal diagrams that should be associated with the suppression of the single-particle density of states.

2.5.2 Quantum critical point (II)

In the vicinity of the transition line, for

$$h = (B - B_c(T))/B_c \ll 1, \quad (2.103)$$

the most singular contribution comes from the lowest LL, $n = 0$. For small temperatures in the vicinity of the Quantum Critical Point (QCP), when

$$t = T/T_c \ll 1, \quad (2.104)$$

we can simplify the inverse fluctuation propagator using the asymptotic formula for the Digamma function:

$$\mathcal{E}_n(\omega) = -h - \ln(2n + 1) - \ln\left(1 - \frac{i\omega}{\epsilon_n}\right). \quad (2.105)$$

In this region, the role of τ_{ϕ} in the fluctuation propagator is mostly to shift the critical magnetic field. We will assume that this shift has already been performed. Besides, it is natural to neglect τ_{ϕ} in the Cooperon, because in the vicinity of the critical

point the Cooperon is not singular and $1/\tau_\phi$ has to compete with Ω_c . Substituting the expression for $\mathcal{E}_n(\omega)$ into Eqs. (2.89)-(2.91) and expanding the propagators in ω/Ω_c , the contributions of all three terms can be written in the form

$$\delta\sigma_{\parallel}^{(i)} = \frac{e^2}{\pi^2} [\alpha^{(i)} I_\alpha(t, h) + \beta^{(i)} I_\beta(t, h)] \quad (2.106)$$

with the numerical coefficients

$$\alpha^{(dos)} = -1, \quad \alpha^{(an)} = 0, \quad \alpha^{(sc)} = \frac{1}{3}, \quad (2.107)$$

$$\beta^{(dos)} = -1, \quad \beta^{(an)} = 2, \quad \beta^{(sc)} = \frac{5}{3}. \quad (2.108)$$

Here

$$I_\alpha = \int_0^{\Omega_c} \frac{\omega \mathcal{B}(\omega) d\omega}{\omega^2 + (h\Omega_c/2)^2}, \quad I_\beta = - \int_0^\infty \frac{\omega^2 \mathcal{B}'(\omega) d\omega}{\omega^2 + (h\Omega_c/2)^2}.$$

Evaluating these integrals, we obtain:

$$I_\alpha(t, h) = \ln \frac{r}{h} - \frac{1}{2r} - \psi(r), \quad (2.109)$$

$$I_\beta(t, h) = r\psi'(r) - \frac{1}{2r} - 1 \quad (2.110)$$

with

$$r = \frac{1}{2\gamma} \frac{h}{t}. \quad (2.111)$$

Note that when all the contributions are summed up, we get $\alpha = -\frac{2}{3}$, $\beta = \frac{8}{3}$, and our result reproduces the one obtained by Galitski and Larkin[30].

The region of the phase diagram in the vicinity of the *QCP* can further be subdivided into classical and quantum regions, depending on the ratio of the parameters

h and t . The superconducting fluctuations contribute either as classically populated modes or through virtual transitions. In the quantum region $t \ll h$ the occupation number of the lowest LL of the collective mode is small, and we obtain

$$\delta\sigma_{\parallel} = -\frac{2e^2}{3\pi^2} \ln \frac{1}{h}, \quad (t \ll h). \quad (2.112)$$

In the classical region $t \gg h$, the occupation number is large and the correction changes its character. As a result, it becomes positive:

$$\delta\sigma_{\parallel} = \frac{2e^2\gamma}{\pi^2} \frac{t}{h}, \quad (t \gg h). \quad (2.113)$$

2.5.3 High temperatures (III) and high magnetic fields (IV)

In these regions the dominant contributions come from high LLs and, hence, the summation in the LL index can be replaced by an integration. At the same time, the full dependence of the fluctuation propagators on the bosonic frequency should be kept, because the leading contribution comes from a long double logarithmic integration.

Let us first discuss the region (III). We will perform the calculation in the limit of $\ln(T/T_c) \gg 1$. We start with the analysis of $\delta\sigma_{\parallel}^{(dos)}$. It has a very slow temperature dependence due to the long integration in energy, which has to be cut off at $\omega, \epsilon \sim \tau^{-1}$, where the diffusive approximation breaks down. In view of this fact, only the term proportional to \mathcal{B} (rather than \mathcal{B}') gives the leading contribution, and we can

write

$$\begin{aligned}
\delta\sigma_{\parallel}^{(dos)} &= \frac{e^2}{4\pi^2} \int \mathcal{B}(\omega) \operatorname{Im} [L^R(\omega) \psi^{R''}(\omega)] d\omega d\epsilon \\
&= -\frac{e^2}{4\pi^2} \operatorname{Im} \int \frac{\mathcal{B}(\omega) \partial_{\omega}^2 \psi \left(\frac{1}{2} + \frac{\epsilon - i\omega}{4\pi T} \right) d\omega d\epsilon}{\ln T/T_c + \psi \left(\frac{1}{2} + \frac{\epsilon - i\omega}{4\pi T} \right) - \psi \left(\frac{1}{2} \right)}.
\end{aligned} \tag{2.114}$$

This integral is logarithmically divergent. As a result, we obtain:

$$\delta\sigma_{\parallel}^{dos} = -\frac{e^2}{2\pi^2} \ln \frac{\ln 1/T_c \tau}{\ln T/T_c}. \tag{2.115}$$

This correction is similar to the Altshuler-Aronov corrections, but with a scale-dependent coupling constant. This result was first derived by Altshuler et al. [9]. At very large temperatures ($\ln T/T_c \gg 1$) this term dominates the total correction. In the case of a repulsive interaction, it becomes [27] $\frac{e^2}{2\pi^2} \ln \ln \frac{1}{T\tau}$.

Let us turn to $\delta\sigma_{\parallel}^{(sc)}$. The term proportional to \mathcal{B}' is again small, $\mathcal{O}(\ln^{-2}(T/T_c))$. Another term, which is proportional to \mathcal{B} , is more important:

$$\delta\sigma_{\parallel}^{(sc)} = e^2 \int_0^{\infty} \frac{izdz}{256\pi^5} \int_{-\infty}^{\infty} \frac{dy \coth \frac{y}{2} \psi'(\epsilon) \psi''(\epsilon)}{[\ln T/T_c + \psi(\epsilon)]^2} \tag{2.116}$$

where $\epsilon = \frac{1}{2} + \frac{z-iy}{4\pi}$. We first calculate the y integral neglecting y in the denominator. Since only $y \gtrsim 1$ contribute to the leading term, we can substitute $\coth \frac{y}{2} \rightarrow \operatorname{sign} y$. This leads to

$$\delta\sigma_{\parallel}^{(sc)} = \frac{e^2}{64\pi^4} \int_0^{\infty} \frac{zdz [\psi' \left(\frac{1}{2} + \frac{z}{4\pi} \right)]^2}{[\ln T/T_c + \psi \left(\frac{1}{2} + \frac{z}{4\pi} \right)]^2}. \tag{2.117}$$

The remaining integral comes from $1 \lesssim z$ and can be calculated to give:

$$\delta\sigma_{\parallel}^{(sc)} = \frac{e^2}{4\pi^2} \frac{1}{\ln T/T_c}. \tag{2.118}$$

We note, however, that the same term originates from the subleading contribution to $\delta\sigma_{\parallel}^{(dos)}$, but with a different numerical coefficient $\frac{\ln 2 - 1}{2\pi^2}$. Thus, different contributions of the kind $\mathcal{O}(\ln^{-1} T/T_c)$ do not cancel each other.

Let us now turn to $\delta\sigma_{\parallel}^{(an)}$. In the continuous limit, $v \sum_n \rightarrow \sum_q$, Eq. (2.90) reproduces the known result[13]. In the limit of $\ln T/T_c \gg 1$, it can be further simplified to:

$$\delta\sigma_{\parallel}^{(an)} = -\frac{e^2}{16\pi^2} \frac{1}{\ln^2 T/T_c} \int_0^{\infty} \frac{M(z) dz}{z + 1/(T\tau_{\phi})} \quad (2.119)$$

with

$$M(z) = \int_{-\infty}^{\infty} \frac{dy \left[\psi\left(\frac{1}{2} + \frac{z-iy}{4\pi}\right) - \psi\left(\frac{1}{2} + \frac{z+iy}{4\pi}\right) \right]^2}{\sinh^2(y/2)}. \quad (2.120)$$

Although this term is formally $\mathcal{O}(\ln^{-2} T/T_c)$, it can still be essential due to the logarithmic divergence at small momenta as it can be seen from Eq. (2.119). With logarithmic accuracy, we can calculate it as follows:

$$\delta\sigma_{\parallel}^{(an)} = -\frac{e^2}{16\pi^2} \frac{1}{\ln^2 T/T_c} \int_0^1 \frac{M(0) dz}{z + 1/(T\tau_{\phi})}. \quad (2.121)$$

As a result, we get:

$$\delta\sigma_{\parallel}^{(an)} = \frac{e^2}{12} \frac{\ln T\tau_{\phi}}{\ln^2 T/T_c}. \quad (2.122)$$

One should keep in mind, however, that τ_{ϕ} itself depends on T . In this region, the anomalous Maki-Thompson correction was considered by several authors, who all obtained the same functional form but with different numerical coefficients[9, 32, 68]. We believe this discrepancy is due to different approximations used for the calculation of $M(0)$.

For high magnetic fields (region (IV)), the situation is to some extent analogous to region (III) with the main difference that the anomalous MT term does not contribute as it is suppressed at small temperature. The dominant corrections originate from

$\delta\sigma^{(sc)}$ and $\delta\sigma^{(dos)}$, and the leading contributions are those which are proportional to $\mathcal{B} \approx \text{sign } \omega$. To proceed, we write the equilibrium propagator in its zero-temperature form:

$$L^{R(A)} = \ln^{-1} \left(\frac{\Omega_c/2h}{\epsilon_n \mp i\omega} \right), \quad (T \rightarrow 0). \quad (2.123)$$

After the frequency integration, we find that $\delta\sigma_{\parallel}^{(dos)}$ takes the following form:

$$\delta\sigma_{\parallel}^{(dos)} = \frac{e^2}{\pi^2} h \sum_n \text{li} \left(\frac{1}{h(2n+1)} \right) \quad (2.124)$$

with the logarithmic integral function $\text{li}(z) = \int_0^z dt/\ln t$. This sum is logarithmically divergent at the upper limit and has to be cut off when the diffusion approximation breaks down, that is at $n \sim N_{max} \gg 1$ with $N_{max} = \frac{1}{hT_c\tau}$. Under these conditions, the sum is dominated by large n and can be found to equal

$$\delta\sigma_{\parallel}^{(dos)} = -\frac{e^2}{2\pi^2} \ln \frac{\ln 1/\tau T_c}{\ln B/B_c}. \quad (2.125)$$

This concludes our discussion of the regions (I-IV) in the phase diagram; the corresponding asymptotic expressions are referenced in Fig. 2.2.

The results we obtained differ from those given in Ref. [32]. This follows from a comparison of the asymptotic behavior in several regions. The most drastic difference, however, concerns the temperature dependence of the resistance for magnetic fields $B > B_c$. The authors of Ref. [32] claimed that for small temperatures $T \ll T_c$ the resistance first increases with increasing T and starts to diminish at $T/T_c \gtrsim (B - B_c)/B_c$. As follows from our asymptotic expressions presented in Eqs. (2.106) and from the result of the numerical calculation shown in Figs. 2.2 and 2.3, the situation is opposite. At a fixed magnetic field, the resistance decreases as

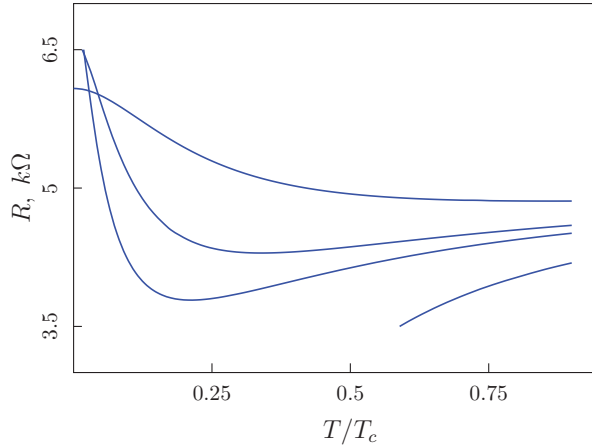


Figure 2.3: Resistance as a function of temperature for magnetic fields $B/B_c = 0.9, 1.05, 1.1, 1.3$. The sample parameters are $R_D = 5k\Omega$ and $T_c\tau = 10^{-2}$.

the temperature increases from zero until the line $\partial_T\sigma = 0$ is crossed. Then the resistance starts to grow.

2.6 Conclusion

We considered homogeneously disordered films above the superconducting transition $T > T_c(B)$ and calculated corrections to longitudinal as well as transversal conductivities. Our results are presented by equations (2.89)-(2.91). We analyzed the asymptotic behavior of these corrections in different regions of the phase diagram and provided a comparison with previously published results.

The results for the longitudinal conductivity, Eqs. (2.89)-(2.91), can be useful for the analysis of experiments. They allow for a complete numerical evaluation of the fluctuation corrections to conductivity without any additional approximation, e.g., the lowest Landau level approximation. Exemplary results are presented in Figs. 2.3, 3.1 for the resistivity $R = (R_D^{-1} + \delta\sigma)^{-1}$ as a function of magnetic field and temperature. A similar behavior of the resistance was observed in the experiment of

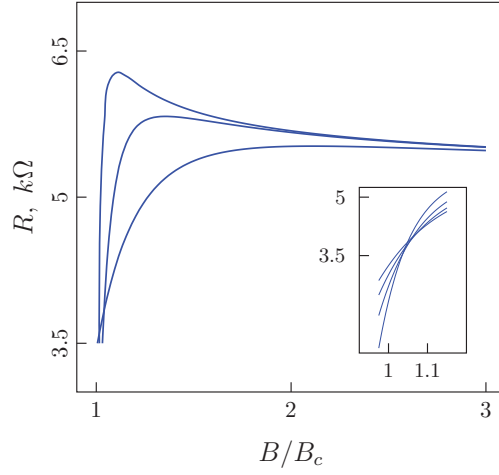


Figure 2.4: Resistance as a function of magnetic field for temperatures $T/T_c = 0.03, 0.1, 0.35$. Inset: the zoomed region of the approximate crossing for $T/T_c = 0.15 - 0.3$. The sample parameters are $R_D = 5k\Omega$ and $T_c\tau = 10^{-2}$.

Baturina et al.[14]. In Ref. [14], the authors presented a fit to the measured data that was based on the asymptotic expressions (2.106) derived in Ref. [30] and reproduced in our work based on a different method. We note, however, that although these expressions provide a good approximation in the vicinity of the QCP, their region of validity does not extend up to the relatively large temperatures and magnetic fields that were considered in the experiment (up to $0.35T_c$ and up to $5B_c$, correspondingly). When fitting this data, the more precise Eqs. (2.89)-(2.91) should, therefore, be used.

According to the results presented in this work, the resistance curves drawn as a function of the magnetic field exhibit an approximate crossing point for a finite interval of temperatures, as demonstrated in Fig. 2.3. As can be seen from this picture, the curves do not literally cross in a single point, but deviations from this ideal behavior are small. The existence of this approximate crossing point is a consequence of a relatively wide minimum in the $R(T)$ curve for $B = 1.05B_c$ as shown in Fig. 2.3. This type of behavior has been observed in several systems; see e.g. Fig. 4

in Ref. [63]. However, in these experiments the curves continue to cross even at the smallest temperatures, while we did not find this kind of behavior from the Gaussian corrections to conductivity. This could be related to the fact that for such low temperatures the proximity to the QCP becomes of crucial importance, and the present theory is not sufficient because 1) it does not account for the effect of non-Gaussian fluctuations and 2) does not take into account the smearing of the transition by disorder[42, 31], which is usually observed in this region (see Fig. 2 in Ref. [38] as an example).

To conclude, we have developed an approach to the calculation of fluctuation conductivity based on the Usadel equation and valid for both the classical as well as the quantum fluctuation regime for arbitrary magnetic fields. This approach is more physically transparent than conventional perturbation theory based on the Kubo formula and provides a bridge between the phenomenological theory and microscopics. We believe that it may find applications in studies of fluctuation effects out of equilibrium or in hybrid superconductor/normal metal structures. Our results for the Hall effect have recently been used in the description of experimental data by Breznay et. al[20] and will be discussed in more details in the following chapter.

3. HALL EFFECT IN SUPERCONDUCTING FILMS*

3.1 Introduction

Measurements of the Hall effect in the classically weak magnetic fields provide useful information about the density of the current carriers as well as the sign of their charge. According to the Drude formulas, the ratio between the Hall (σ_{xy}) and longitudinal (σ_{xx}) conductivities is $\omega_c\tau$, where $\omega_c = eH/m^*c$ is the cyclotron frequency of the quasiparticles (electrons or holes) and τ is the elastic scattering time. The appearance of the cyclotron frequency in the expression for σ_{xy} manifests the fact that for the Hall effect to be finite particle-hole asymmetry is required. Within the Drude model the Hall coefficient is independent of τ and ω_c , and is only function of the charge carriers density n ; $R_H \equiv \rho_{xy}/H = 1/nec$. Weak localization corrections arising due to the interference effects although modifying both σ_{xy} and σ_{xx} leave R_H unchanged. In contrast, electron-electron interactions affect the transverse and longitudinal components of the conductivity tensor in a way violating the balance between them and R_H is no longer universal. In particular, a significant change in the Hall coefficient occurs near the superconducting transition as a result of the electron-electron interaction in the Cooper channel which finally leads to the onset of superconductivity. As we show below, the corrections to the Hall conductivity due to superconducting fluctuations diverge stronger than the longitudinal ones in the vicinity of the thermal phase transition and as strong as longitudinal ones in the vicinity of the quantum (magnetic field-driven) phase transition. Furthermore, the

*Part of this chapter is reprinted with permission from "Fluctuation conductivity in disordered superconducting films" by K. S. Tikhonov, G. Schwiete, A. M. Finkel'stein, 2012, Physical Review B 85 (17), 174527, Copyright (2012) by the American Physical Society and "Hall effect in superconducting films" by K. Michaeli, K. S. Tikhonov, A. M. Finkel'stein Physical Review B 86 (1), 014515, Copyright (2012) by the American Physical Society.

particle-hole asymmetry factor $\omega_c\tau$ is multiplied by $\varsigma\mu$ that makes it parametrically larger. The parameter ς is proportional to the derivative of the density of states with respect to the energy at the chemical potential μ .

Similar to the Hall conductivity of free electrons, the corrections to σ_{xy} generated by the superconducting fluctuations vanish in the absence of particle-hole asymmetry. Close to T_c , the superconducting fluctuations can be described using the time dependent Ginzburg-Landau (TDGL) [71, 2, 35] equation:

$$-\frac{\pi/8}{T_c} \left(\frac{\partial}{\partial t} + 2ie\varphi \right) \Delta(\mathbf{r}, t) = \left[\frac{T - T_c}{T_c} + \frac{\pi D}{8T_c} (-i\nabla - 2e\mathbf{A})^2 \right] \Delta(\mathbf{r}, t). \quad (3.1)$$

As was discussed in the previous section, the TDGL-equation can be derived directly from the microscopic theory by integrating out the single-particle degrees of freedom. Then, under the assumption that the quasiparticles have a constant density of states, one arrives to Eq. 3.1. Eq. 3.1 is thus invariant under particle-hole transformation. Therefore, the contribution of the superconducting fluctuations to the Hall conductivity vanishes in the framework of this equation. It has been first pointed out by Fukuyama *et al.* [28] that the Aslamazov-Larkin correction vanishes unless the derivative of the density of states with respect to the energy is taken into account. In other words, this contribution to the Hall conductivity depends on the particle-hole asymmetry. This important observation was the basis for subsequent studies of the Hall effect in the framework of TDGL theory both for conventional and high- T_c superconductors as well as in the flux-flow regimes. [23, 84, 87].

Aronov *et al.* [10, 11] incorporated the particle-hole asymmetry into the TDGL equation by adding a new term:

$$-\left(\frac{\partial}{\partial t} + 2ie\varphi \right) \left(\frac{a}{T_c} + i\varsigma \right) \Delta(\mathbf{r}, t) = \left[\frac{T - T_c}{T_c} + \frac{\pi D}{8T_c} (-i\nabla - 2e\mathbf{A})^2 \right] \Delta(\mathbf{r}, t). \quad (3.2)$$

This equation was used to derive the Aslamazov-Larkin correction to the Hall conductivity. The authors of Ref. [10] claimed that the new parameter, can be related to the derivative of the critical temperature with respect to the chemical potential, $\varsigma = -0.5d \ln T_c/d\mu \sim -\lambda^{-1}\nu'(\mu)/\nu(\mu)$. Here λ is the dimensional coupling constant determining $T_c = \omega_D \exp(-1/\lambda)$, and $\nu(\mu)$ is the density of states at the Fermi energy while $\nu'(\mu)$ is its derivative with respect to the energy. Hence, the corrections to the Hall conductivity, being proportional to ς , can provide information on the dependence of the density of states on the energy. Microscopic calculation presented below confirms that for three dimensional electrons ς is proportional to $1/(\lambda\varepsilon_F)$. The analysis of Eq. 3.2 reveals that in the diffusive regime the cyclotron frequency corresponding to the charged field Δ is equal to $\Omega_c = |4eHD/c|$, where $\Omega_c \propto (\varepsilon_F\tau)\omega_c \gg \omega_c$. In Ω_c , the effective charge is equal to $2e$ and the diffusion coefficient D replaces $1/2m$, because in the fluctuation propagators the kinetic energy $p^2/2m$ is substituted by Dq^2 . Consequently, the Drude-like contribution of the superconducting fluctuations to the Hall conductivity is proportional to $\varsigma\Omega_c$.

Here we extend previous theoretical analysis [28, 10, 11] of the the corrections to the Hall conductivity for various temperatures and magnetic fields. Although the diagonal component of the magnetoresistance has been studied for the entire phase diagram including the vicinity of the Quantum Critical Point, induced by magnetic field [30], see also a previous section, up to now there was no similar systematic analysis of the Hall resistance. As we explained above, the particle-hole asymmetry enters the Hall conductivity either via the quasiparticle mass (or equivalently, the cyclotron frequency ω_c) or the derivative of the density of states. While the former appears when the Lorentz force acts on the quasiparticles in order to turn the current from the longitudinal to the transverse direction, the latter appears when the Lorentz force acts on the superconducting fluctuations. Thus, in general, there are two

distinct types of corrections to the Hall conductivity, one proportional to $\omega_c\tau$ and the other to $\varsigma\Omega_c \sim \omega_c\tau/\lambda$. Since the coupling constant for the superconducting interaction is usually much smaller than unity, one may expect only the second kind of contributions to be important. This fact allows for self-consistent treatment of the problem in the quasiclassical approximation.

3.2 Particle-hole asymmetry and superconducting fluctuations

Let us discuss the contribution to Hall conductivity that arises due to the deflection of the fluctuating supercurrent. In order to calculate it, it is enough to modify the superconducting fluctuation propagator according to [10]

$$L_{R(A)}^{-1}(\omega) \rightarrow L_{R(A)}^{-1}(\omega) - \varsigma\omega. \quad (3.3)$$

As a consequence of the additional term, the superconducting propagators lose their particle/hole symmetry, i.e., the relation $L^A(-\omega) = L^R(\omega)$ no longer holds. In the framework of the BCS theory, the asymmetry parameter ς can be related to the energy dependence of the density of states at the Fermi level: $\varsigma = -\frac{1}{2\lambda} \frac{d\ln\nu}{d\mu}$ or, equivalently[10], to the variation of T_c with the chemical potential: $\varsigma = -\frac{1}{2} \frac{d\ln T_c}{d\mu}$. In the simple model of 3D electrons with a quadratic spectrum, one has $\nu(\epsilon) \approx \nu_0(1 + \epsilon/2\epsilon_F)$ and $\varsigma = -1/(4\epsilon_F\lambda)$. For $\lambda \ll 1$ the contributions arising from $\delta\sigma_{\perp}^{(sc)}$ are parametrically larger than those arising from $\delta\sigma_{\perp}^{(dos)}$ and $\delta\sigma_{\perp}^{(an)}$. In our calculation of the Hall conductivity, we work in the framework of the quasiclassical approach, using, however, Eq. (3.3) for the propagators $L_{R(A)}$. This is a consistent procedure that allows to obtain all contributions to the transverse current proportional to the large parameter $1/\lambda$.

Here we will explain the mechanism of appearance of the parameter ς in the propagator of superconducting fluctuations given in Eq. 3.3. For that we calculate

\hat{L} taking into account the dependence of the density of states and velocity of the quasiparticles on energy. In the normal state, the quasiparticles are described in terms of the Fermi liquid theory where the standard approximation is to consider the density of states and velocity in the vicinity of the Fermi energy as constants. The dependence of the Fermi liquid parameters on energy leads only to small corrections and can be usually ignored. However, under this approximation the propagator of superconducting fluctuations satisfies $L^R(\omega) = L^A(-\omega)$ and, consequently, the fluctuations corrections to the Hall effect vanish. Therefore, when studying the Hall effect, we have to go beyond the Fermi liquid approximation. Note that although the fluctuations in superconducting films are effectively two-dimensional, the quasiparticles in a not too thin film are still three-dimensional and, hence, the density of states ν is not a constant.

The propagator of superconducting fluctuations at equilibrium can be found from the polarization operator. As we study effects of superconducting fluctuations in the gaussian approximation, the disorder-averaged polarization operator can be written in terms of the Cooperon and the quasiparticle Green's functions. Before proceeding, we note that in our approximation it will be enough to find Π in the absence of magnetic field, and reintroduce the magnetic field in the end. Then, the calculation can be done in momentum and frequency space, and the Cooperon becomes:

$$C^R(\mathbf{q}, \epsilon, \omega - \epsilon) = \left[1 - V_{\text{imp}}^2 \int \frac{d\mathbf{k}}{(2\pi)^3} g^R(\mathbf{k}, \epsilon) g^A(\mathbf{q} - \mathbf{k}, \omega - \epsilon) \right]^{-1}. \quad (3.4)$$

The particle-hole asymmetry enters the calculation of the Cooperon in numerous ways. Although the asymmetry affects also the Cooperon, in the derivation of the corrections to the Hall conductivity we neglected it. Including the dependence of the Cooperon on the particle-hole asymmetry leads to corrections which are smaller

by a factor $T\tau \ll 1$ or $1/\varepsilon_F\tau \ll 1$ than the terms discussed here. First of all, the non-constant density of states affects the elastic scattering time, and hence, modifies the quasiparticle Green's function:

$$g^{R,A}(\mathbf{k}, \epsilon) = [\epsilon - \xi_{\mathbf{k}} \pm i\pi V_{\text{imp}}^2 \nu(\epsilon)]^{-1}. \quad (3.5)$$

For a parabolic spectrum of three-dimensional quasiparticles, $\nu(\epsilon) \approx \nu_0(1 + \epsilon/2\varepsilon_F)$. Similarly, the integration over the momentum in Eq. 3.4, is sensitive to the energy dependence of the density of states and velocity. In practice, however, the analysis of the leading contribution shows that only the modification of the quasiparticle Green's functions are important. Then, expanding the density of states in the Green's functions, one gets:

$$C^{R,A}(\mathbf{q}, \epsilon, \omega - \epsilon) = \frac{1 + \omega/4\varepsilon_F}{\mp i(2\epsilon - \omega)\tau + Dq^2\tau}, \quad (3.6)$$

where $\tau = (2\pi V_{\text{imp}}^2 \nu_0)^{-1}$ is the elastic scattering time at the Fermi energy calculated in the Born approximation.

We can see that the particle-hole asymmetry modifies the Cooperon by the factor $(1 + \omega/4\varepsilon_F)$. Correspondingly, the polarization operator becomes:

$$\Pi^{R,A}(\mathbf{q}, \omega) = - \left(1 + \frac{\omega}{4\varepsilon_F}\right) \left[\psi \left(\frac{1}{2} + \frac{\mp i\omega + Dq^2}{4\pi T} \right) - \psi \left(\frac{1}{2} \right) + \ln \frac{T}{T_c} - \frac{1}{\lambda} \right]. \quad (3.7)$$

Not too far from the superconducting transition, we can write the propagator

$L^{R,A}(\mathbf{q}, \omega)$ to the leading corrections due to the particle-hole asymmetry as:

$$\begin{aligned}
L^{R,A}(\mathbf{q}, \omega) &= -\frac{1}{\nu_0} \left\{ \frac{1}{\lambda} + \left(1 + \frac{\omega}{4\varepsilon}\right) \left[\ln \frac{T}{T_c} + \psi \left(\frac{1}{2} + \frac{\mp i\omega + Dq^2}{4\pi T} \right) - \psi \left(\frac{1}{2} \right) - \frac{1}{\lambda} \right] \right\}^{-1} \\
&\approx \frac{-1}{\nu_0} \left[\ln \frac{T}{T_c} + \psi \left(\frac{1}{2} + \frac{\mp i\omega + Dq^2}{4\pi T} \right) - \psi \left(\frac{1}{2} \right) - \frac{\omega}{4\varepsilon_F \lambda} \right]^{-1}.
\end{aligned}
\tag{3.8}$$

Defining $\varsigma = -1/4\varepsilon_F \lambda$, we get the expression for the propagator of the superconducting fluctuations used in the main text (see Eq. 3.3). The asymmetry parameter ς can be rewritten as $\varsigma = -0.5d \ln T_c / d \ln \mu$, in accordance with Ref [10]. Furthermore, in the presence of magnetic field, the term Dq^2 in the propagator L (as well as in the Cooperon) is quantized into the Landau levels, $Dq^2 \rightarrow \Omega_c(N + 1/2)$. One may still use the obtained value for the parameter ς in the propagator L as given in Eq. 3.3 for the analysis of fluctuation effects in the Hall conductivity in the whole region T - H of the superconducting transition, $T = T_c(H)$.

3.3 Discussion of the results for Hall conductivity due to superconducting fluctuations

We proceed with the discussion of the results for the transverse conductivity presented in Eq. (2.91). These expressions represent only those contributions to $\delta\sigma_{\perp}$, which describe a deflection of the supercurrent. In principle other contributions exist, in which quasiparticles are deflected in the transverse direction by the Lorentz force. These contributions are not included in the approximation we apply here. The terms not accounted for by Eq. (2.91) include the contribution due to the anomalous MT process, discussed by Fukuyama et al.[28] and the contribution $\delta\sigma_{\perp}^{(dos)}$, recently discovered diagrammatically by Michaeli et al.[61], which is reminiscent of the density of state suppression. They are related to the corresponding corrections to the

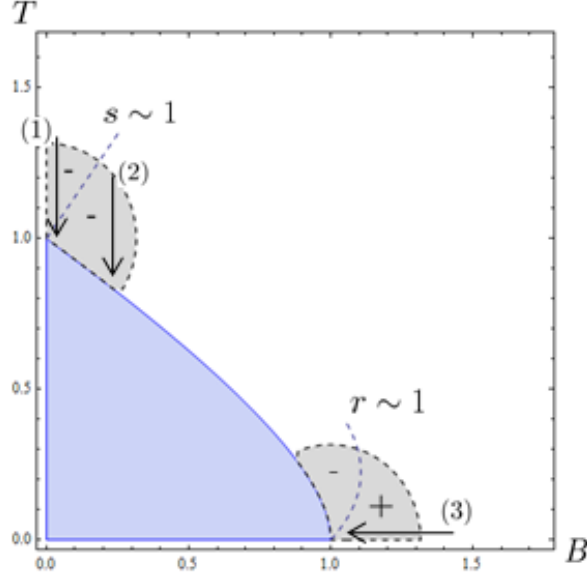


Figure 3.1: Phase diagram for the Hall effect: sign of the fluctuation correction to σ_{xy} coefficient is shown.

longitudinal conductivity as follows:

$$\delta\sigma_{\perp}^{(an)} = -2\omega_c\tau\delta\sigma_{\parallel}^{(an)}, \quad (3.9)$$

$$\delta\sigma_{\perp}^{(dos)} = -\frac{\omega_c\tau}{2}\delta\sigma_{\parallel}^{(dos)}. \quad (3.10)$$

Note, that $\delta\sigma_{\perp}^{(an)}$ and $\delta\sigma_{\parallel}^{(an)}$ cancel each other in the expression for the Hall resistivity $\rho_{xy} = -\sigma_{xy}/(\sigma_{xx}^2 + \sigma_{xy}^2) \approx -\sigma_{xy}/\sigma_{xx}^2$. In contrast, the DOS-corrections give a finite contribution to ρ_{xy} .

In region (I) after expansion in $\Omega_c(n+1/2)/4\pi T$ and $\omega/4\pi T$ the correction $\delta\sigma_{\perp}^{(sc)}$ takes the form

$$\delta\sigma_{\perp}^{(sc)} = -\frac{16e^2\zeta\Omega_c(T\tau_{GL})^2}{\pi^2}f(s), \quad (3.11)$$

where

$$f(s) = s^2 \left[1 + \psi\left(\frac{1}{2} + s\right) - \psi(1+s) - s\psi'(1+s) \right].$$

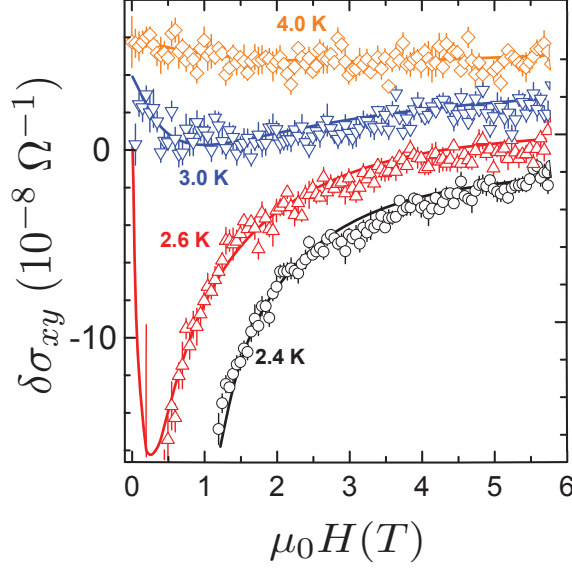


Figure 3.2: Hall effect in the superconducting films: experiment and theory.

In this region, the Hall effect can be considered phenomenologically: the same expression (3.11) was obtained by Aronov and Rapoport[11] (with a different coefficient, it has later been corrected by Aronov et al.[10]) on the basis of the time dependent Ginzburg-Landau theory. For $s \gg 1$, when quantization of the LLs for the superconducting fluctuations is negligible, the expression (3.11) becomes:[28]

$$\delta\sigma_{\perp}^{(sc)} = \frac{e^2\zeta\Omega_c}{96} \left(\frac{T}{T - T_c} \right)^2. \quad (3.12)$$

The region of applicability of the Eq. (3.11) is in fact very narrow, and already for $T \gtrsim 1.01T_c$ one should not expand the full expression for $\delta\sigma_{\perp}^{(sc)}$ in $\Omega_c(n + 1/2)/4\pi T$ to get an accurate result. The corresponding formula has been given in Ref. [61]:

$$\delta\sigma_{\perp}^{(sc)} = \frac{2e^2\zeta T}{\pi} \sum_n (n + 1) \frac{[L_{n+1}^R(0) - L_n^R(0)]^3}{[L_{n+1}^R(0) + L_n^R(0)]^2}. \quad (3.13)$$

In region (II), we can limit ourselves to the lowest LL and follow the same route as in the calculation of the longitudinal conductivity. This gives for the quantum regime:

$$\delta\sigma_{\perp}^{(sc)} = -\frac{e^2\zeta\Omega_c}{3\pi^2} \ln \frac{1}{h}, \quad (3.14)$$

and for the classical regime:

$$\delta\sigma_{\perp}^{(sc)} = \frac{2e^2}{\pi} \frac{\zeta T}{h}. \quad (3.15)$$

Note, that in this region $\delta\sigma_{\perp}^{(dos)}$ and $\delta\sigma_{\perp}^{(an)}$ exhibit the same singular behavior as $\delta\sigma_{\perp}^{(sc)}$. We do not provide the corresponding expressions, since they follow straightforwardly from Eqs. (3.9) and (3.10), together with Eq. (2.106).

3.4 Conclusion

To conclude, we have calculated fluctuation corrections to the Hall conductivity coefficient σ_{xy} due to superconducting fluctuations. Most of these results are new (only results for 'classical' region for weak magnetic fields were known before). We have analyzed asymptotic behaviour of these corrections in different regions of the phase diagram and compared our results with previously published in full details.

Our theoretical results for Hall coefficient have recently been used for description of experiments by Stanford group [20]. The experimental data together with the curves, obtained with the use of the results, described above (with only one fitting parameter - diffusion coefficient) are shown on the Figure 3.2.

4. TRANSVERSE SPIN SEEBECK EFFECT*

4.1 Introduction

The key and most intriguing effect among the spin-dependent effects in spin caloritronics [82, 43, 44, 83, 6, 81, 26, 21, 15]. is the transverse spin Seebeck effect (SSE) in which a thermal gradient in a ferromagnet/substrate structure gives rise to spin-currents which vary along the length of the sample and are detected via the inverse spin-Hall voltage[86]. This effect has been experimentally observed using different ferromagnetic materials: metals,[82] semiconductors,[43, 44] and insulators.[83] The magnitude of the SSE is quantified by the transport coefficient $S_{xy} = \frac{V_y}{w\nabla_x T}$, where V_y is the measured ISHE voltage, w is the width of Pt probe, and $\nabla_x T = (T_2 - T_1)/L$, where L is the length of the sample, see Fig. 4.1. The ISHE voltage is given by $V_y = \frac{2|e|\rho\theta_H}{\hbar}(\mathbf{j}_s \times \mathbf{s})_y$, where \mathbf{j}_s is the spin current, \mathbf{s} is its polarization, θ_H is the spin-Hall angle of the probe (in Pt, θ_H is of the order of one per cent) and ρ is its electric resistivity. The effect is non-local, *i.e.* it depends on the position along the sample rather than the local temperature gradient. In addition, the size of the sample is usually about 1 *cm* and such a long-ranged information about position can be transferred only by phonons, propagating along the insulating substrate.[43] The key role of phonons for the transverse SSE effect was discussed in the Ref. [6].

Here we show that the non-locality of the SSE is a consequence of the non-local energy transfer due to sub-thermal diffusive phonons that are sensitive to the boundary conditions and give rise to a spectral non-uniform temperature along the sample.[56, 54] In fact, in recent measurements in bilayer F-Pt wire devices, the spe-

*Part of this chapter is reprinted with permission from "Spectral non-uniform temperature and non-local heat transfer in the spin Seebeck effect" by K. S. Tikhonov, J. Sinova, A. M. Finkel'stein, 2013, Nature Communications 4, Copyright (2013) by the Nature Publishing Group.

cific geometry excludes long-ranged propagation of magnons and leaves only phonons as a source of non-locality.[81] In addition, we demonstrate that while in the insulator the SSE is likely determined by the phonon-magnon mechanism, in the conducting ferromagnet (e.g., Ni₈₁Fe₁₉[82] and GaMnAs[44]), the magnon mechanism is not the only one available. The experiments by Jaworski *et al.* in Ref. [44] were performed on a material with Curie temperature $T_C = 130$ K, considerably lower than the Debye temperature $\theta_D = 350$ K, and showed that $V_{\text{ISHE}} \propto M$ at the vicinity of the Curie point; i.e. the SSE signal vanishes with the magnetization M with the same critical behavior. This latter fact excludes the magnon mechanism for this case: as we have checked, starting from Eq. (12) of the Ref. [5], the magnon pumping yields the contribution to the SSE signal, which vanishes as $M^{3/2}$.

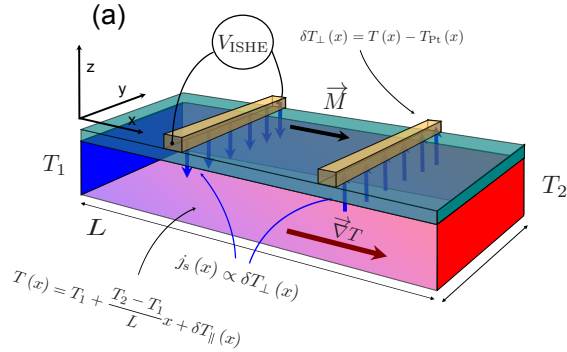


Figure 4.1: Scheme of the SSE experiment. The effect incorporates three key physical mechanisms: (i) subthermal phonons whose inelastic length, l_{in} , is of the order of the sample size, L , and whose elastic length, l_{el} , is smaller than L , drive the non-local heat propagation along the substrate which gives rise to a steady state distribution function that deviates from local equilibrium; (ii) equilibration of heat flows out of the substrate into the Pt probe and backwards establishes the temperature in the probe $T_{\text{Pt}} \neq T(x)$; (iii) the different phonon distribution functions in the probe and the substrate yield a spin-phonon-drag current, $\vec{j}_s(x) \propto \delta T_{\perp}$.

In order to evaluate the dependence of the spin current (pumped by a magnon

mechanism) on the average magnetization M , we start from the Eq. 12 of the Ref. 15. The spin current is then given by (with magnon damping neglected):

$$C = I_s/\Delta T \propto J_{sd}^2 M^2 \tau_{sf} \int \frac{J_{\mathbf{k}-\mathbf{q}} d^3 \mathbf{k} d^3 \mathbf{q}}{(1 + \lambda_N^2 \mathbf{k}^2)^2 + (\omega_{\mathbf{q}} \tau_{sf})^2} B(\omega_{\mathbf{q}}/T) \propto \\ \propto J_{sd}^2 M^2 \tau_{sf} \int \frac{d\mathbf{q}_z d\mathbf{k}_z d^2 \mathbf{n}}{(1 + \lambda_N^2 (\mathbf{k}_z^2 + \mathbf{n}^2))^2 + (M (\mathbf{q}_z^2 + \mathbf{n}^2) \tau_{sf})^2} B(M (\mathbf{q}_z^2 + \mathbf{n}^2) / T)$$

with

$$B(z) = \frac{z^2}{\sinh^2 z}.$$

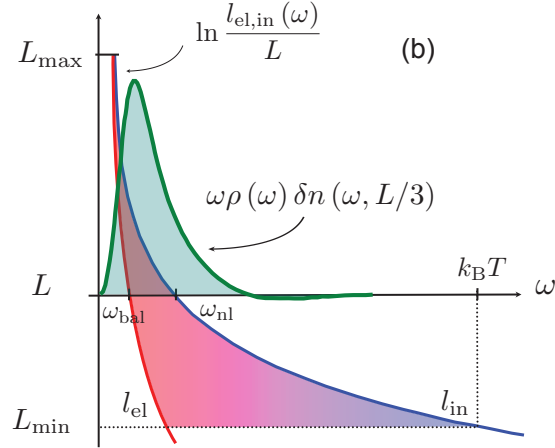


Figure 4.2: Spectral phase diagram of phonons as a function of sample length. The deviation from local thermal equilibrium, $\delta n(\omega, x) = n(\omega, x) - n_{T(x)}(\omega)$, is illustrated (green curve) for $x = L/3$; here $\rho_{\text{ph}}(\omega) \propto \omega^2$ is the phonon density of states.

We have taken into account the magnon dispersion law $\omega_{\mathbf{q}} = M\mathbf{q}^2$, and the form of interaction J , which conserves in-plane momentum:

$$\mathbf{k} = \mathbf{n} + \mathbf{k}_z, \quad \mathbf{q} = \mathbf{n} + \mathbf{q}_z.$$

Writing

$$\lambda_N k_z = a, \quad M q_z^2 / T = b^2, \quad M n^2 / T = c^2$$

we obtain:

$$C \propto J_{sd}^2 M^2 \tau_{sf} \frac{(T/M)^{3/2}}{\lambda_N} F(q_T \lambda_N, T \tau_{sf}),$$

where $q_T = \sqrt{T/M}$ is a thermal magnon wavevector and function $F(\xi, \gamma)$ equals

$$F(\xi, \gamma) = \int \frac{B(b^2 + c^2) c d c d b d a}{(1 + a^2 + c^2 \xi^2)^2 + (b^2 + c^2)^2 \gamma^2}.$$

This function behaves as follows:

$$F(\xi \gg \gamma \gg 1) \propto \xi^{-2},$$

giving in this limit $C \propto M^{3/2}$.

4.2 Physical mechanisms of the phonon-electron SSE

The theory of this phonon-electron SSE, which does not involve magnons, has three key physical mechanisms. The first (i) involves the non-local nature of the signal driven by subthermal phonons, which is also relevant for the magnon-phonon mechanism not considered here. In recent measurements of the SSE in insulators[7] the temperature difference between thermal magnons and phonons assumed in the current theory[91, 5] has not been observed, suggesting the necessity of the concept of spectrally non-uniform temperature. This concept originates from the fact that in most dielectrics, and also some semiconductors, the energy transfer is highly non-

local[56, 54] because of the strong dependence of the diffusion coefficient of phonons on frequency: $D(\omega) \propto \omega^{-4}$, if the dominant scatterers are point-like.[94] In the diffusive regime of the experiments the energy relaxation length is given by $l_{\text{in}}(\omega) = \sqrt{D(\omega) \tau_{\text{in}}(\omega)}$, where the energy relaxation rate is $\tau_{\text{in}}^{-1}(T, \omega) \propto T^4 \omega$. While the thermal phonons, $\hbar\omega \sim k_B T$, are equilibrated, the subthermal low-frequency phonons can deviate from the local equilibrium due to the rapid low-frequency growth of inelastic length $l_{\text{in}}(\omega) = l_{\text{in}}(T) (T/\omega)^{5/2}$, which leads to non-local kinetics. Even the concept of temperature itself is well-defined only for phonons of high enough frequency. For the 'thermal' part of the spectrum $\hbar\omega \gtrsim k_B T$, the distribution function has a Planckian form $n_T(\omega) = (e^{\hbar\omega/k_B T} - 1)^{-1}$ with a local temperature $T = T(x)$. As a result, the phonons which store the energy and phonons which transfer it are located in different parts of the spectrum. As illustrated in Fig. 4.2, this spectral separation occurs when $l_{\text{el}}(T) \ll l_{\text{in}}(T) \ll L$, where $l_{\text{el}}(T) \equiv l_{\text{el}}(\hbar\omega = k_B T) \propto D(\hbar\omega = k_B T) \propto T^{-4}$, and $l_{\text{in}}(T) \equiv l_{\text{in}}(\hbar\omega = k_B T) \propto T^{-4.5}$. Then the subthermal phonons whose inelastic length is of the order of (but whose elastic length is much shorter) than L drive the non-local heat propagation along the substrate, giving rise to a steady state phonon distribution function that deviates from local equilibrium for $\hbar\omega \ll k_B T$ and depends on the position along the substrate. This deviation from local thermal equilibrium in the low frequencies manifest in a $T(x)$ profile which deviates from a linear dependence. To describe this non-local effect, it is essential to formulate the boundary conditions for the equations describing the propagation of the diffusive phonons. [Previously[91], the sensitivity to the boundaries entered the theory as a result of the different boundary conditions imposed on phonons and magnons[69]. This model, however, cannot explain the position dependence of the SSE signal, measured on the sample with scratched magnet[43] or on the bilayer wire device.[81] Here, instead, we demonstrate that phonons in different parts of the energy spectrum act as the

”subsystems” of different sensitivity to the boundaries.]

The second (ii) mechanism involves the electron-phonon drag. Since the probe is a ’dead end’, there is a full balance between incoming and outgoing heat fluxes such that net heat flux is zero. However, the incoming and outgoing fluxes have different spectral distributions, because of the inelastic processes in Pt which average out the spectrum of the incoming flux, and establish a local temperature $T_{\text{Pt}}(x)$ different from $T(x)$. The spin drag, induced by the phonon flux, is sensitive to the spectral content of the phonon distribution function. Hence, despite zero net heat flux, the spin injection is not zero. In the stationary situation, the drag voltage induced by the phonons is compensated by redistribution of the electron density, so that the total electric current is zero (as well as electrochemical potential gradient). However, in the presence of a spin polarization, there will be a net spin current $j_s = j_\uparrow - j_\downarrow$ polarized along magnetization M : unlike its charge counterpart, spin drag is not blocked by accumulation of the spin density, which is eliminated by SO interaction in Pt. The magnitude of j_s depends on the ratio of the thickness of the ferromagnet, d_F , and the phonon inelastic scattering length there, l_{in}^F . The optimal value of d_F for observing the phonon drag SSE is of the order of $l_{\text{in}}^F(T)$. For too thin ferromagnet, $d_F \ll l_{\text{in}}^F$, the phonons cannot effectively transfer their momentum to electrons to drag them toward the probe. In the opposite limit, $d_F \gg l_{\text{in}}^F$, the phonons equilibrate before they reach the region near the probe. An alternative mechanism not considered here is the quantum acoustoelectric pumping[55] due to the spectrally non-uniform flux of phonons.

The final (iii) mechanism involves the conversion of the spin-current to an electric signal via the ISHE. This conversion is most optimal if the thickness of the Pt layer is of the same order of magnitude as the spin relaxation length in Pt, which is the case in the discussed experiments.[93] As shown in detail in the following sections,

the resulting theory gives the correct magnitude of the signal, predicts a dependence on magnetization $S_{SSE} \propto M$, and gives specific temperature and size dependencies that can be tested experimentally.

4.3 Subthermal phonon kinetics

On Fig. 4.2 we show the spectral phase diagram of frequency regions contributing differently to the kinetics of phonons. There are two characteristic frequencies, ω_{nl} and ω_{bal} , determining the propagation of phonons:

$$l_{in}(\omega_{nl}) = L, \quad l_{el}(\omega_{bal}) = L. \quad (4.1)$$

For non-local transport we require $\hbar\omega_{nl} = k_B T (L/l_{in}(T))^{-2/5} \ll k_B T$. In addition, we will not be interested in phonons in the ballistic part of the spectrum, $\omega < \omega_{bal}$. This is legitimate as long as $\omega_{bal} \ll \omega_{nl}$, and determines a maximum length of the sample, L_{max} , given by the point of intersection of the curves $l_{in}(\omega)$ and $l_{el}(\omega)$, as shown Fig. 4.2). This gives a temperature dependence $L_{max} \propto T^{-16/3}$. For lengths larger than L_{max} , the non-local effect is due to the fraction of phonons propagating ballistically and requires a different formalism, which we will not discuss here. The other condition that allows to separate thermal phonons from those which produce non-local effects is $l_{in}(T) \ll L$. This gives a minimum length of the sample $L_{min} \propto T^{-9/2}$. For length smaller than L_{min} even thermal phonons are out of equilibrium and spectral separation does not hold. The large ratio of $l_{in}(T)/l_{el}(T)$ opens the window $L_{min} \ll L \ll L_{max}$, which we are interested in. Hence the sample size should be in the range indicated on Fig. 4.2. Estimation at $T = 10$ K (when typical phonon energy is 28 K), gives L_{max} about few *cm* and L_{min} on the scale of *mm*. Recall that the typical size of the sample used for the SSE experiments is 1*cm*. With temperature the width of the region of applicability of the theory behaves as $L_{max}/L_{min} \propto T^{-5/6}$

and we expect it to be relevant up to 50K. In addition, the temperature is assumed to be much smaller than the Debye temperature, $T \ll \theta_D$, which allows us to ignore Umklapp processes.

With these specific length restrictions we consider next the theory of propagation of diffusive phonons along the substrate. Owing to the fact that the low-frequency phonons do not primarily interact with themselves but with equilibrated high-frequency phonons, one may use the following kinetic equation that describes propagation of phonons in the insulating substrate, valid for $\hbar\omega \lesssim k_B T$:

$$D(\omega) \partial_x^2 n(\omega, x) = \frac{\delta n(\omega, x)}{\tau_{\text{in}}(\omega)}, \quad (4.2)$$

where δn is the deviation from the local equilibrium

$$\delta n(\omega, x) = n(\omega, x) - n_{T(x)}(\omega). \quad (4.3)$$

The solution to this second order differential equation requires two sets of effective boundary condition equations. The first, which establishes $T(x)$ from a given $\delta n(x, \omega)$, is obtained from continuity of the energy density in the system, which in stationary situations reads as $\nabla \cdot \vec{j}_Q = 0$.

Because of the divergence of $D(\omega)$ at small ω , the heat flux \vec{j}_Q is transported by the low-energy part of the spectrum.[64, 66, 39] The heat current density is given by:

$$\vec{j}_Q(x) = - \int_0^\infty \hbar\omega \rho_{\text{ph}}(\omega) D(\omega) \partial_x n(\omega, x) d\omega, \quad (4.4)$$

where $\rho_{\text{ph}}(\omega) \propto \omega^2$ is the phonon density of states (summed over all branches). The integral for $\vec{j}_Q(x)$ diverges and has to be cut off at small frequency (the exact value of the cut off does not enter our results since the integral for $\nabla \cdot \vec{j}_Q$ converges). Using

Eq. (4.2), the energy density continuity equation takes the following form:

$$\int_0^\infty \omega^2 \delta n(\omega, x) \rho_{\text{ph}}(\omega) d\omega = 0. \quad (4.5)$$

This equation should hold for all x . Thus, one has to solve a system of integro-differential equations. For the case of a pulse propagation in an infinite media the non-local phonon transport has been studied in Ref. [56, 54, 90]. However, we are interested in a stationary solution in the presence of the boundaries which yield the second equation that fully establishes $n(\omega, x)$ and $T(x)$.

On the boundary between the substrate and the heater there is a jump in the phonon distribution function, because of the abrupt change in the properties of materials. This leads to a finite thermal boundary resistance (Kapitza resistance), which manifests itself through the jump ΔT_K at the contact.[76] If the scattering in the vicinity of the boundary is mostly elastic, the boundary condition consists of conservation of spectral heat current density across the boundary. It relates the heat flux through the boundary to the jump of the phonon distribution function across it. At the left end of the sample (which is at heat contact with a reservoir at temperature T_1) it takes the following form:

$$l_{\text{el}}(\omega) \partial_x n(\omega, x)|_{x=0} = \frac{1}{R_{\text{Bd}}} [n(\omega, 0) - n_{T_1}(\omega)]. \quad (4.6)$$

The boundary resistance R_{Bd} is assumed to be frequency independent. If the heat contacts are in thermal equilibrium, R_{Bd} can be related to the thermal boundary conductivity $h_{\text{Bd}} = \frac{\dot{Q}}{A\Delta T_K} \propto \frac{T^3}{v_s^2} R_{\text{Bd}}^{-1}$, where v_s is the averaged sound velocity. Note, that in the absence of the boundary resistance ($R_{\text{Bd}} = 0$), the locally equilibrated distribution function $n(\omega, x) = n_{T_0(x)}(\omega)$ with $T_0(x) = T_1 + (T_2 - T_1)x/L$ satisfies

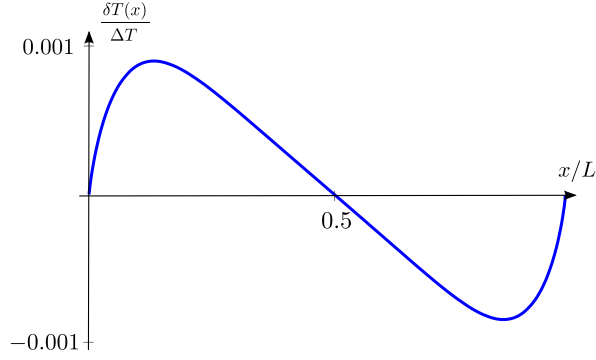


Figure 4.3: Correction to the linear temperature dependence as a function of position, Eq. (4.12).

the kinetic equation, so that $\delta n = 0$ and the non-local effect vanishes since the boundaries are effectively at infinity. One may easily see that $\delta n \propto R_{\text{Bd}}$ at not too large values of R_{Bd} .

With this it is then possible to write down a closed equation for $T(x)$. If the phonon temperature as a function of position x is known, the distribution function can be obtained from Eq. (4.2) and reads:

$$n(\omega, x) = n^{\text{S}}(\omega, x) + Z_{\omega} \int \Pi_{\omega}(L - x_{<}) \Pi_{\omega}(x_{>}) n_{T(x')}(\omega) dx' / l_{\text{in}}(\omega) \quad (4.7)$$

where $x_{<} = \min(x, x')$, $x_{>} = \max(x, x')$. The 'source' term $n^{\text{S}}(\omega, x)$ comes from the boundary condition (4.6) and is equal to

$$n^{\text{S}}(\omega, x) = g_{\omega} Z_{\omega} [n_{T_1}(\omega) \Pi_{\omega}(x) + n_{T_2}(\omega) \Pi_{\omega}(L - x)], \quad (4.8)$$

where

$$\Pi_{\omega}(x) = \cosh\left(\frac{L - x}{l_{\text{in}}(\omega)}\right) + g_{\omega} \sinh\left(\frac{L - x}{l_{\text{in}}(\omega)}\right), \quad (4.9)$$

and

$$Z_\omega = [2g_\omega \cosh(L/l_{\text{in}}(\omega)) + (1 + g_\omega^2) \sinh(L/l_{\text{in}}(\omega))]^{-1}. \quad (4.10)$$

Above we have introduced the effective boundary thermal conductance $g_\omega = (l_{\text{in}}(\omega)/l_{\text{el}}(\omega)) R_{\text{Bd}}^{-1}$. The second term in Eq. (4.7) describes the process of redistribution of phonons along the sample due to diffusion and inelastic scattering. Substituting Eq. (4.7) into Eq. (4.5), one gets an integral equation for $T(x)$, which can be solved numerically. This procedure is self-consistent: after finding $T(x)$, the distribution function is easily calculated from Eq. (4.7). To illustrate the result, we assume the following ratios of characteristic lengths of a thermal phonon

$$L : l_{\text{in}}(T) : l_{\text{el}}(T) = 1 : 0.1 : 0.005, \quad (4.11)$$

and calculate the correction $\delta T_{\parallel}(x)$ to the linear temperature behavior

$$T(x) = T_1 + \frac{T_2 - T_1}{L}x + \delta T_{\parallel}(x), \quad (4.12)$$

which is shown on Fig. 4.3, where we have assumed that $R_{\text{Bd}} = 0.1$ and $T_1 < T_2$. Although the deviation from the linear behaviour is small, it ensures the conservation of the energy density of the phonons propagating along the substrate. Ultimately, the non-equilibrium correction $\delta n(\omega, x)$ is responsible for the SSE effect. On Fig. 4.2, the frequency dependence of $\hbar\omega\rho_{\text{ph}}(\omega)\delta n(\omega, x)$ is plotted close to the colder end (for $x = 0.3L$). On the hotter end, δn has the opposite sign.

4.4 Out of plane spin transport

After finding the non-equilibrium distribution function of phonons $\delta n(\omega, x)$, we next concentrate on the heat and spin transport in the vertical direction from the

substrate to the probe across the magnet. The temperature of phonons in the Pt probe, $T_{Pt}(x)$, is different from the $T(x)$. It is determined by the requirement that the heat flux created by non-equilibrium non-local phonons from the substrate to Pt is compensated by back-flow flux of thermal phonons from Pt to the substrate. The resulting temperature difference, $\delta T_{\perp}(x) = T(x) - T_{Pt}(x)$, can be found from the heat balance equation:

$$\int_0^{\infty} \omega \rho_{\text{ph}}(\omega) \delta N(\omega, x) d\omega = 0, \quad (4.13)$$

where $\delta N(\omega, x) = n_{\text{sub}} - n_{\text{Pt}}$ is the difference of the distribution function of phonons entering and leaving the Pt probe, located at x . Here we neglect inelastic scattering of phonons while they pass through the ferromagnetic layer ($d_{\text{F}} \lesssim l_{\text{in}}^{\text{F}}$), and have assumed the sound velocities to be of similar order in the Pt and the substrate. We also assume, that the probe is small enough $a \ll l_{\text{el}}(T)$, so that the influence of the counterflow on the phonon distribution function in the substrate can be ignored.

It is useful to present $\delta N(\omega, x)$ in the following form:

$$\delta N(\omega, x) = [n_{T(x)}(\omega) - n_{T_{Pt}(x)}(\omega)] + \delta n(\omega, x). \quad (4.14)$$

Then, the the temperature difference $\delta T_{\perp}(x)$ can be calculated from the equation:

$$\delta T_{\perp}(x)/T(x) \propto - \int_0^{\infty} z^3 \delta n(zT, x) dz \equiv -h(x), \quad (4.15)$$

where $h(x)$ is the dimensionless heat flux supplied to the probe by the nonequilibrium phonons. The function $h(x)$ can be written in a form of $h(x) = \frac{\Delta T}{T} (\omega_{\text{bal}}/T)^4 H(x)$, where $H(x)$ is a slow function of temperature and boundary resistance R_{Bd} . Here ω_{bal} encodes information about scattering of phonons on the disorder and the length

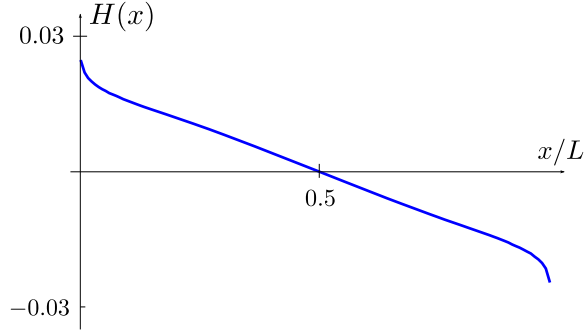


Figure 4.4: The function $H(x) \propto \delta T_{\perp}(x)$ determining the magnitude and spatial profile of the SSE signal S_{xy} given in Eq. (4.20).

of the sample. Function $H(x)$ is plotted on Fig. 4.4 for the same sample parameters as before.

With this we can finally estimate the scale of the SSE due to conducting electrons, dragged by out-of-equilibrium phonons, in more detail. The guiding idea about the scale of the effect follows from the derivation of the well known Gurevich formula[36, 17, 57] for the phonon drag. This formula gives for thermoelectric coefficient $\eta = -j/\nabla T$ the following expression: $\eta \propto -\frac{\sigma T^3}{e(p_F v_s)^3}$, which is valid when $q_T l \gg 1$ (here $q_T = k_B T/\hbar v_s$ is the wavevector of a thermal phonon). For the dirty case $q_T l \ll 1$, the particle current density dragged to the probe is given by [72]:

$$j_e^z(x) \propto \frac{\tau_{ei}}{p_F} \int_0^{\infty} \omega^2 \delta N(\omega, x) W(\omega l_{ei}/v_s) \rho_{ph}(\omega) d\omega. \quad (4.16)$$

We write τ_{ei} , l_{ei} for electron-impurity scattering time and length in the ferromagnet. The role of electron-impurity scattering in Eq. (4.16) is twofold. It enhances electron-phonon interaction by slowing the motion of electrons (making it diffusive). This is taken into account by the form of $W(x)$. On the other hand it diminishes the drag effect due to the loss of electron momentum by impurity scattering. The details of

the function $W(x)$ depend on the character of the scattering of phonons on defects. We assume that phonons scatter on impurities vibrating with the lattice[65] and $W(x) = W_{\text{vb}}(x)$. For temperatures $k_{\text{B}}T \ll \hbar v_{\text{s}}/l_{\text{ei}}$, we may use the asymptotic behavior $W_{\text{vb}}(x \ll 1) \approx x$. Recalling that the charge current will be compensated by an unpolarized backflow charge current from the Pt probe, the total spin current is given by the polarized current dragged by the phonons into the Pt probe. Finally, we rewrite the expression for the spin-phonon-drag current injected into the Pt probe as

$$j_{\text{s}}^z(x) \propto X_{\text{M}} T (T/v_{\text{s}})^2 (T/\theta_{\text{D}})^2 A_{\text{el}}(T) J(x, T), \quad (4.17)$$

where $A_{\text{el}}(T) = (k_{\text{B}}T/\epsilon_{\text{F}}) (k_{\text{F}}l_{\text{ei}})^2$ is a dimensionless constant, determined by electrons, $X_{\text{M}} = \frac{n_{\uparrow} - n_{\downarrow}}{n_{\uparrow} + n_{\downarrow}}$ is the level of spin polarization and the dragging factor is

$$J(x, T) = \int_0^{\infty} z^5 \delta N(zT, x) dz. \quad (4.18)$$

Since the spectral densities of the energy and the charge currents are proportional to different powers of the phonon frequency, the electronic drag due to phonons is possible even when the net energy flow is zero. The contribution to J in Eq. (4.18) arising due to the temperature difference $\delta T_{\perp}(x)$ between the substrate and the Pt probe (first term in Eq. (4.14)) is dominant. In other words, while the non-locality of the effect along the sample is carried by the low-frequency phonons, the dragging force generating the spin-current is produced by the thermal phonons. As a result of this intricate joint effort by the phonons in different parts of the spectrum, one gets (restoring units):

$$j_{\text{s}}^z(x) = X_{\text{M}} (k_{\text{B}}/\hbar)^3 A_{\text{el}}(T) (T/\theta_{\text{D}})^2 (T/v_{\text{s}})^2 \delta T_{\perp}(x). \quad (4.19)$$

Finally, for the magnitude of the SEE, $S_{xy} = -2(|e|\rho/\hbar)\theta_H j_s^z/\nabla_x T$, and recalling that $\delta T_\perp(x) \propto -Th(x)$, we obtain:

$$S_{xy} = \theta_H S_{xy}^{(0)} A_{\text{el}}(T) X_M k_F l_{\text{el}} (\theta_D/2.8) H(x), \quad (4.20)$$

where $S_{xy}^{(0)} = |e|k_F\rho$ is a material-dependent constant. The factor 2.8 takes into consideration that the energy of thermal phonon is $2.8k_B T$. Assuming that in Pt, $\rho = 0.9 \mu\Omega \cdot m$ and $k_F^{-1} = 10^{-8} cm$, we obtain $S_{xy}^{(0)} \approx 30 \mu V K^{-1}$. Function $H(x)$ is positive at the cold end, meaning the dragging force pushes electrons towards the magnet there, according to Eq. (4.19). Note that although the electron-phonon drag is proportional to a high power of temperature, see Eq. (4.17), the final result for the SSE coefficient is only weakly temperature dependent, $S_{xy} \propto T$. It comes out as a result of the strong dispersion of the phonon scattering time in the substrate. Although function $H(x)$ in Eq. (4.20) is also temperature dependent, this dependence comes only from the non-locality of the phonon collision integral in energy, and is relatively weak. Another important property of this function is that its spatial profile varies with temperature rather slowly. This is because the phonons which contribute mostly to the non-local effect have inelastic scattering length of the order of the sample size. Varying the temperature mainly results in the shift of the relevant phonon energy ω_{nl} , so that the corresponding length scale $l_{\text{in}}(\omega_{\text{nl}})$ remains the same. These observations stress the importance of the strong dispersion of the phonon scattering.

Taking $\theta_H = 0.08$, $\epsilon_F/k_B = 10^3 K$, $\theta_D = 350 K$, $k_F l_{\text{ei}} = 10$ and the ratio of characteristic lengths as in (4.11), we find the magnitude of the effect at $10 K$ to be $S \sim 20 \mu V K^{-1} \times X_M$.

4.5 Conclusion

In this work we have discussed the main ingredients of the phonon dynamics in the substrate that allows to understand the spatial profile of the SSE signal. As we have shown, to explain the non-local effect, *i.e.* its dependence on the position of the probe along the substrate, one must consider the spectral non-uniformity of the phonon distribution function which can be interpreted as spectrally non-uniform temperature. A key aspect of the non-locality is the explicit introduction of the boundaries into the equations describing the propagation of diffusing phonons.

In addition, we have presented a scheme of the non-magnon mechanism in the case when the ferromagnetic element of the device is conducting and obtain the correct magnitude of the effect. (The recent observation[41] of the magnetic proximity effect in FM/Pt contact suggests the possibility of another channel to contribute to the SSE voltage: anomalous Nernst effect. However, it is less universal than the electron-phonon drag and in any case must rely on the mechanism which we propose for generation of the non-local signal: subthermal phonons with energy dispersive diffusion, which is quite universal.)

Furthermore, the spatial profile of the SSE signal, presented in Fig. 4.4, is very similar to the one shown as a 'universal' profile on the Fig. 2f of the Ref. [43]. Although the phonon kinetics at temperatures comparable with θ_D is strongly modified by Umklapp processes, the measured proportionality between the SSE signal and the magnitude of the magnetization in Ref. [44] clearly indicates that near $T_C \approx 130$ K the effect is still dominated by the flux of the spin-polarized electrons, instead of the magnon-mediated spin torque. We believe that the difference between the data presented in Figs 2 and 3 of Ref. [44] - in particular, the difference in the behavior near the T_C , - supports this picture. Two different samples demonstrate drastically dif-

ferent temperature behavior. The sample which is thicker and grown on a substrate of a better quality has larger peak value of both S_{xy} and thermopower α_{xx} and also much faster decay of S_{xy} at approaching T_C . The stronger thermopower observed in the thicker sample demonstrates that in this sample phonons lose momentum mainly in collisions with electrons, while in the thinner sample, their scattering on the defects is more efficient. However, due to strong sensitivity of the phonon distribution function at the F-Pt boundary to the ratio $d_F/l_{in}^F(T)$, in the thicker sample the SSE decays with temperature much faster than in the thinner one. As we have already discussed, at large $d_F/l_{in}^F(T)$ the phonons equilibrate before they reach the probe. Indeed, in the thicker sample (more than three times thicker than the thinner one) the effect was not even resolved near the Curie temperature within the accuracy of the measurement. This suggests the need to study the dependence of the SSE signal on the thickness of the magnetic sample in otherwise identical conditions, *i.e.*, keeping the properties of the insulating substrate and semiconductor/substrate boundary the same.

As some direction of the future work, it is interesting to note another manifestation of similar physics, as was recently probed in experiments by the Ohio group. Before this recent experiment, SSE was thought to exist only in magnetic materials. However, in paper [45], the detection of a thermally driven spin current in a wire made of indium antimonide (InSb) was reported, which has even symmetry (the voltage retains its sign) under reversal of the magnetic-field direction $\mathbf{B} \rightarrow -\mathbf{B}$. In fact, we believe that Jaworski et al. show that magnetic field is not even needed to observe the spin Seebeck effect at all as the signal survives down to $\mathbf{B} = 0$, while being strongly enhanced in quantizing fields leading to the spin Seebeck coefficient which was up to 1,000 times larger than that observed in previous measurements of the similar effect in magnetic materials. The authors argue that their finding is

the result of an interplay of: (i) spin imbalance in a magnetic field which is especially strong in InSb, (ii) absence of equilibrium between the electrons and phonons maintained over the sample size, and (iii) strong electron-phonon interaction.

In the spirit of the experiment, discussed in previous chapter, this new version of the spin Seebeck effect is a finite-size effect. The voltage probes 'knows' whether it is located at the hot or the cold end of the sample. What is really new in this experiment (apart from the unusually large magnitude of S_{xy}) is the signal's (almost) even symmetry in \mathbf{B} , which contrasts the symmetry found in magnetic systems. We believe that it indicates a different mechanism of generation of the transversal current and shows that spin Seebeck effect is even more general than previously believed. It is probable that a broken crystallographic symmetry together with the spin-orbit interaction, is the origin of the transversal current in the new setup. We leave this question for the future studies.

5. SUMMARY

In this thesis we have discussed the theories of two transverse effects based on the diffusion-type kinetic equations.

First, we have demonstrated how the Hall effect due to superconducting fluctuations can be described in the framework of the Usadel equation with fluctuating sources as long as superconducting coupling can be considered weak ($\lambda \ll 1$). Our results are valid in the vicinity of both thermal and quantum phase transitions as well as in the crossover regime and thus can be very useful for accurate description of amorphous superconducting films

Second, we have shown that Transverse Spin Seebeck Effect can be understood as a direct manifestation of elastic diffusive propagation of low-energy phonons in insulators. We demonstrated that strong dispersion of the phononic elastic scattering rate leads to quite specific predictions which can be directly probed in experiments. In particular, the proposed mechanism predicts the shape of the position dependence of the transverse Seebeck voltage along the sample to be temperature-independent in a relatively wide temperature window. Recent experimental results are qualitatively consistent with this mechanism, but detailed quantitative description would require further studies.

REFERENCES

- [1] E. Abrahams, R. E. Prange, and M. J. Stephen. Effect of a magnetic field on fluctuations above T_c . *Physica*, 55:230–233, 1971.
- [2] Elihu Abrahams and Toshihiko Tsuneto. Time variation of the ginzburg-landau order parameter. *Physical Review*, 152(1):416, 1966.
- [3] M. Abramowitz and I. Stegun. *Handbook of Mathematical Functions*. Dover Publ. NY, 1972.
- [4] A. A. Abrikosov, L. P. Gor'kov, and I. E. Dzyaloshinski. *Methods of Quantum Field Theory in Statistical Physics*. Prentice-Hall, Inc. Englewood Cliffs, New-Jersey, 1963.
- [5] Hiroto Adachi, Jun-ichiro Ohe, Saburo Takahashi, and Sadamichi Maekawa. Linear-response theory of spin seebeck effect in ferromagnetic insulators. *Physical Review B*, 83(9):094410, 2011.
- [6] Hiroto Adachi, Ken Uchida, Eiji Saitoh, Jun Ohe, Saburo Takahashi, and Sadamichi Maekawa. Gigantic enhancement of spin seebeck effect by phonon drag. *Applied Physics Letters*, 97(25):252506, 2010.
- [7] M. Agrawal, V.I. Vasyuchka, A.D. Karenowska, A.A. Serga, G.A. Melkov, and B. Hillebrands. Magnon-phonon coupling unmasked: a direct measurement of magnon temperature. *arXiv preprint arXiv:1209.3405*, 2012.
- [8] B. L. Altshuler, A. G. Aronov, and D. E. Khmel'nitsky. Effects of electron-electron collisions with small energy transfers on quantum localisation. *Journal of Physics C*, 15:7367, 1982.

- [9] B. L. Altshuler, A. Varlamov, and M. Yu. Reizer. Electron-interaction effects and conductivity of disordered two-dimensional systems. *Zh. Eksp. Theor. Fiz.*, 84:2280–2289, 1983.
- [10] A. G. Aronov, S. Hikami, and A. I. Larkin. Gauge invariance and transport properties in superconductors above T_c . *Phys. Rev. B*, 51(6):3880, 1995.
- [11] A. G. Aronov and A. B. Rapoport. Hall effect in superconductors above T_c . *Mod. Phys. Lett. B*, 6(16-17):1083, 1992.
- [12] L. G. Aslamazov and A. I. Larkin. Effect of fluctuations on the properties of a superconductor above the critical temperature. *Fiz. Tverd. Tela*, 10:1104, 1968.
- [13] L. G. Aslamazov and A. A. Varlamov. Fluctuation conductivity in intercalated superconductors. *Journal of Low Temperature Physics*, 38:223–241, 1980.
- [14] T. I. Baturina, J. Bentner, C. Strunk, M. R. Baklanov, and A Satta. From quantum corrections to magnetic-field-tuned superconductor-insulator quantum phase transition in tin films. *Physica B*, 359(0):500 – 502, 2005.
- [15] Gerrit E W Bauer, Eiji Saitoh, and Bart J van Wees. Spin caloritronics. *Nature materials*, 11(5):391–9, May 2012.
- [16] W. Belzig, F. K. Wilhelm, C. Bruder, G. Schön, and A. D. Zaikin. Quasiclassical green’s function approach to mesoscopic superconductivity. *Superlattices Microstruct.*, 25(5-6):1251–1288, 1999.
- [17] F.J. Blatt, P.A. Schroeder, C.L. Foiles, and D. Greig. *Thermoelectric power of metals*. Plenum Press New York, 1976.
- [18] W. Brenig, M. C. Chang, E. Abrahams, and P. Wölfle. Inelastic scattering time above the superconductivity transition in two dimensions: Dependence on disorder and magnetic field. *Phys. Rev. B*, 31:7001–7005, 1985.

- [19] W. Brenig, M. A. Paalanen, A. F. Hebard, and P. Wölfle. Magnetoconductance of thin-film superconductors near critical disorder. *Phys. Rev. B*, 33:1691–1699, Feb 1986.
- [20] Nicholas P Breznay, Karen Michaeli, Konstantin S Tikhonov, Alexander M Finkel’stein, Mihir Tendulkar, and Aharon Kapitulnik. Hall conductivity dominated by fluctuations near the superconducting transition in disordered thin films. *Physical Review B*, 86(1):014514, 2012.
- [21] Marius V Costache, German Bridoux, Ingmar Neumann, and Sergio O Valenzuela. Magnon-drag thermopile. *Nature materials*, 11(3):199–202, March 2012.
- [22] V. V. Dorin, R. A. Klemm, A. A. Varlamov, A. I. Buzdin, and D. V. Livanov. Fluctuation conductivity of layered superconductors in a perpendicular magnetic field. *Phys. Rev. B*, 48:12951–12965, Nov 1993.
- [23] Alan T. Dorsey. Vortex motion and the hall effect in type-ii superconductors: A time-dependent ginzburg-landau theory approach. *Phys. Rev. B*, 46:8376–8392, Oct 1992.
- [24] G. Eilenberger. Transformation of gorkov’s equation for type ii superconductors into transport-like equations. *Z. Phys.*, 214:195–213, 1968.
- [25] M. V. Feigel’man, A. I. Larkin, and M. A. Skvortsov. Keldysh action for disordered superconductors. *Phys. Rev. B*, 61(18):12361–12388, May 2000.
- [26] J Flipse, F L Bakker, A Slachter, F K Dejene, and B J van Wees. Direct observation of the spin-dependent Peltier effect. *Nature nanotechnology*, 7(3):166–8, March 2012.
- [27] H. Fukuyama. *Electron-Electron Interactions in Disordered Systems*. North-Holland Amsterdam, 1985.

- [28] H. Fukuyama, H. Ebisawa, and T. Tsuzuki. Fluctuation of the order parameter and hall effect. *Prog. Theor. Phys*, 46(4):1028–1041, 1971.
- [29] V. M. Galitski and S. Das Sarma. Renormalization of the upper critical field by superconducting fluctuations. *Phys. Rev. B*, 67(14):144501, 2003.
- [30] V. M. Galitski and A. I. Larkin. Superconducting fluctuations at low temperature. *Phys. Rev. B*, 63(17):174506, 2001.
- [31] V. M. Galitski and A. I. Larkin. Galitski and larkin reply:. *Phys. Rev. Lett.*, 89:109704, Aug 2002.
- [32] A. Glatz, A. A. Varlamov, and V. M. Vinokur. Fluctuation spectroscopy of disordered two-dimensional superconductors. *Phys. Rev. B*, 84:104510, Sep 2011.
- [33] A. Glatz, A. A. Varlamov, and V. M. Vinokur. Quantum fluctuations and dynamic clustering of fluctuating cooper pairs. *EPL*, 94:47005, 2011.
- [34] L. P. Gor'kov. Singularities of the resistive state with current in thin superconducting films. *JETP Lett*, 11(1):32–35, 1970.
- [35] LP Gorkov and GM Eliashberg. Generalization of the ginzburg-landau equations for non-stationary problems in the case of alloys with paramagnetic impurities. *SOV PHYS JETP*, 27(2):328–334, 1968.
- [36] L Gurevich. *Zhurnal Eksperimentalnoi I Teoreticheskoi Fiziki*, 16:193, 1946.
- [37] N. Hadacek, M. Sanquer, and J. C. Villégier. Double reentrant superconductor-insulator transition in thin tin films. *Phys. Rev. B*, 69(2):024505, 2004.
- [38] A. F. Hebard and M. A. Paalanen. Pair-breaking model for disorder in two-dimensional superconductors. *Phys. Rev. B*, 30:4063–4066, Oct 1984.
- [39] C. Herring. The role of low-frequency phonons in thermoelectricity and thermal conduction. *Proc. Int. Coll*, 1956.

- [40] S. Hikami and A.I. Larkin. Magnetoresistance of high temperature superconductors. *Mod. Phys. Lett. B*, 2(5):693–698, 1988.
- [41] SY Huang, WG Wang, SF Lee, J Kwo, and CL Chien. Intrinsic spin-dependent thermal transport. *Physical review letters*, 107(21):216604, 2011.
- [42] R. Ikeda. Comment on “disorder and quantum fluctuations in superconducting films in strong magnetic fields”. *Phys. Rev. Lett.*, 89:109703, Aug 2002.
- [43] C. M. Jaworski, J. Yang, S. Mack, D. D. Awschalom, J. P. Heremans, and R. C. Myers. Observation of the spin-seebeck effect in a ferromagnetic semiconductor. *Nature Mat.*, 9:898–903, 2010.
- [44] C. M. Jaworski, J. Yang, S. Mack, D. D. Awschalom, R. C. Myers, and J. P. Heremans. Spin-seebeck effect: A phonon driven spin distribution. *Phys. Rev. Lett.*, 106:186601, May 2011.
- [45] CM Jaworski, RC Myers, E Johnston-Halperin, and JP Heremans. Giant spin seebeck effect in a non-magnetic material. *Nature*, 487(7406):210–213, 2012.
- [46] A. Kamenev and A. Levchenko. Keldysh technique and non-linear σ -model: basic principles and applications. *Adv. in Phys*, 58(3):197–319, 2009.
- [47] N. B. Kopnin. *Theory of Nonequilibrium Superconductivity*. Oxford University Press, New York, 2001.
- [48] N. C. Koshnick, H. Bluhm, M. E. Huber, and K. A. Moler. Fluctuation superconductivity in mesoscopic aluminum rings. *Science*, 318(5855):1440, 2007.
- [49] A. I. Larkin and Y. N. Ovchinnikov. Quasiclassical method in the theory of superconductivity. *Sov. Phys. JETP*, 28(6):1200–1205, 1969.
- [50] A. I. Larkin and Y. N. Ovchinnikov. Influence of inhomogeneities on superconductor properties. *JETP*, 34:651, 1972.

- [51] A. I. Larkin and Y. N. Ovchinnikov. Nonlinear fluctuation phenomena in the transport properties of superconductors. *JETP*, 92(3):519–528, 2001.
- [52] A. I. Larkin and A. A. Varlamov. *Theory of fluctuations in superconductors*, volume 127. Oxford University Press, USA, 2005.
- [53] A. Levchenko and A. Kamenev. Keldysh ginzburg-landau action of fluctuating superconductors. *Phys. Rev. B*, 76(9):094518, Sep 2007.
- [54] Y. Levinson. *Sov. Phys. JETP*, 52(4):704, 1980.
- [55] Y. Levinson, O. Entin-Wohlman, and P. Wölfle. Acoustoelectric current and pumping in a ballistic quantum point contact. *Phys. Rev. Lett.*, 85:634–637, Jul 2000.
- [56] Y.B. Levinson. Nonlocal phonon heat transfer. *Solid State Communications*, 36(1):73 – 75, 1980.
- [57] E.M. Lifshitz, L.P. Pitaevskii, and L.D. Landau. *Physical kinetics*, volume 60. Pergamon press Oxford, 1981.
- [58] W. Liu, M. Kim, G. Sambandamurthy, and N. P. Armitage. Dynamical study of phase fluctuations and their critical slowing down in amorphous superconducting films. *Phys. Rev. B*, 84:024511, Jul 2011.
- [59] A. V. Lopatin, N. Shah, and V. M. Vinokur. Fluctuation conductivity of thin films and nanowires near a parallel-field-tuned superconducting quantum phase transition. *Phys. Rev. Lett.*, 94:037003, Jan 2005.
- [60] K. Maki. The critical fluctuation of the order parameter in type-ii superconductors. *Prog. Theor. Phys*, 39(4):897–906, 1968.
- [61] Karen Michaeli, Konstantin S Tikhonov, and Alexander M Finkel’stein. Hall effect in superconducting films. *Physical Review B*, 86(1):014515, 2012.

- [62] T. Mishonov, A. Posazhennikova, and J. Indekeu. Fluctuation conductivity in superconductors in strong electric fields. *Phys. Rev. B*, 65:064519, Jan 2002.
- [63] M. A. Paalanen, A. F. Hebard, and R. R. Ruel. Low-temperature insulating phases of uniformly disordered two-dimensional superconductors. *Phys. Rev. Lett.*, 69:1604–1607, Sep 1992.
- [64] R. Peierls. *Ann. Phys. (Leipzig)*, 3:1055, 1929.
- [65] A. B. Pippard. *Philos. Mag*, 46:1104, 1955.
- [66] I. Pomeranchuk. On the thermal conductivity of dielectrics. *Physical Review*, 60(11):820, 1941.
- [67] A. Pourret, H. Aubin, J. Lesueur, C. A. Marrache-Kikuchi, L. Berge, L. Dumoulin, and K. Behnia. Observation of the nernst signal generated by fluctuating cooper pairs. *Nature Phys*, 2(10):683–686, 2006.
- [68] M. Yu. Reizer. Fluctuation conductivity above the superconducting transition: Regularization of the maki-thompson term. *Phys. Rev. B*, 45:12949–12958, Jun 1992.
- [69] DJ Sanders and D. Walton. Effect of magnon-phonon thermal relaxation on heat transport by magnons. *Physical Review B*, 15(3):1489, 1977.
- [70] A. Schmid. Diamagnetic susceptibility at the transition to the superconducting state. *Phys. Rev.*, 180:527–529, Apr 1969.
- [71] Albert Schmid. A time dependent ginzburg-landau equation and its application to the problem of resistivity in the mixed state. *Physik der kondensierten Materie*, 5(4):302–317, 1966.
- [72] A. Sergeev and V. Mitin. Effect of electronic disorder on phonon-drag thermopower. *Phys. Rev. B*, 65:064301, Dec 2001.

- [73] Nayana Shah and Andrei Lopatin. Microscopic analysis of the superconducting quantum critical point: Finite-temperature crossovers in transport near a pair-breaking quantum phase transition. *Phys. Rev. B*, 76:094511, Sep 2007.
- [74] H. Smith. Quantum field-theoretical methods in transport theory of metals' j. rammer. *Rev. Mod. Phys.*, 58(2), 1986.
- [75] M. Steiner and A. Kapitulnik. Superconductivity in the insulating phase above the field-tuned superconductorinsulator transition in disordered indium oxide films. *Physica C*, 422(12):16 – 26, 2005.
- [76] ET Swartz and RO Pohl. Thermal boundary resistance. *Reviews of Modern Physics*, 61(3):605, 1989.
- [77] Brian Tarasinski and Georg Schwiete. Fluctuation conductivity of disordered superconductors in magnetic fields. *Phys. Rev. B*, 88:014518, Jul 2013.
- [78] R. S. Thompson. *Phys. Rev. B*, 1:327, 1970.
- [79] Konstantin S Tikhonov, Georg Schwiete, and Alexander M Finkel'stein. Fluctuation conductivity in disordered superconducting films. *Physical Review B*, 85(17):174527, 2012.
- [80] Konstantin S Tikhonov, Jairo Sinova, and Alexander M Finkelstein. Spectral non-uniform temperature and non-local heat transfer in the spin seebeck effect. *Nature communications*, 4, 2013.
- [81] K. Uchida, H. Adachi, T. An, T. Ota, M. Toda, B. Hillebrands, S. Maekawa, and E. Saitoh. Long-range spin seebeck effect and acoustic spin pumping. *Nature Materials*, 10(10):737–741, 2011.

- [82] K. Uchida, S. Takahashi, K. Harii, J. Ieda, W. Koshibae, K. Ando, S. Maekawa, and E. Saitoh. Observation of the spin seebeck effect. *Nature*, 455:778–781, Oct 2008.
- [83] K. Uchida, J. Xiao, H. Adachi, J. Ohe, S. Takahashi, J. Ieda, T. Ota, Y. Kajiwara, H. Umezawa, H. Kawai, G. E. W. Bauer, S. Maekawa, and E. Saitoh. Spin seebeck insulator. *Nature Mat.*, 9:894–897, 2010.
- [84] Salman Ullah and Alan T. Dorsey. Effect of fluctuations on the transport properties of type-ii superconductors in a magnetic field. *Phys. Rev. B*, 44:262–273, Jul 1991.
- [85] K. D. Usadel. Generalized diffusion equation for superconducting alloys. *Physical Review Letters*, 25(8):507–509, 1970.
- [86] S.O. Valenzuela and M. Tinkham. Direct electronic measurement of the spin hall effect. *Nature*, 442(7099):176–179, 2006.
- [87] Anne van Otterlo, Mikhail Feigel'man, Vadim Geshkenbein, and Gianni Blatter. Vortex dynamics and the hall anomaly: A microscopic analysis. *Phys. Rev. Lett.*, 75:3736–3739, Nov 1995.
- [88] A. A. Varlamov and L. Reggiani. Nonlinear fluctuation conductivity of a layered superconductor: Crossover in strong electric fields. *Phys. Rev. B*, 45(2):1060, 1992.
- [89] A. F. Volkov, K. E. Nagaev, and R. Seviour. Fluctuation paraconductivity in mesoscopic superconductor–normal-metal contacts. *Phys. Rev. B*, 57(9):5450–5456, Mar 1998.
- [90] TE Wilson and WL Schaich. A calculation of nonlocal phonon heat transfer. *Solid State Communications*, 50(1):3–6, 1984.

- [91] Jiang Xiao, Gerrit E. W. Bauer, Ken Uchida, Eiji Saitoh, and Sadamichi Maekawa. Theory of magnon-driven spin seebeck effect. *Phys. Rev. B*, 81:214418, Jun 2010.
- [92] G. Zala, B. N. Narozhny, and I. L. Aleiner. Interaction corrections at intermediate temperatures: Magnetoresistance in a parallel field. *Physical Review B*, 65(2):020201, 2001.
- [93] Steven S.-L. Zhang and Shufeng Zhang. Spin convertance at magnetic interfaces. *Phys. Rev. B*, 86:214424, Dec 2012.
- [94] J.M. Ziman. *Electrons and phonons: the theory of transport phenomena in solids*. Oxford University Press, USA, 2001.